The holotype of the basal archosauromorph *Prolacerta broomi* revisited

GABRIELA SOBRAL

Prolacerta broomi is one of the most important of fossil reptiles. First considered as one of the earliest members of squamates, this basal archosauromorph has been used as a model for diapsid morphological evolution ever since its discovery, playing a pivotal role in hypotheses on the origin of diapsid reptiles. The holotype of *Prolacerta broomi* (UCMZ 2003.41R) is known from a mostly complete skull, but the original description is limited to the superficial features of the skull roof and palate. Since then, many other specimens of *Prolacerta broomi* have been recovered that potentially account for this limited access to anatomical information, but it remains unclear whether these aspects correspond well to the known material of the holotype. Here, the skull morphology of the holotype of *Prolacerta broomi* is revisited through the use of μCT scans. The identifications of some cranial elements have been corrected, such as the left prefrontal and lacrimal, and several new elements are revealed, including the epi- and ectopterygoids, prearticular, coronoid, and braincase bones. The orbitonasal region is described in detail and significantly shows a contribution of the lacrimal to the dorsal alveolar canal. Finally, the addition of the holotype as an independent OTU in recently published analyses indicate conflicts with the current knowledge on *Prolacerta broomi* phylogenetic affinity and taxonomy. First, it points to potential taxonomic inconsistency since the holotype does not form a monophyletic group with other *Prolacerta broomi* OTUs in any of the analyses and, second, it suggests a more basal position for the holotype than that recovered in some studies, more basal than rhynchosaurs and close to the origin of Crocopoda. Together, these findings indicate areas of future research interest in the study of early evolving archosauromorphs.

Key words: Reptilia, Diapsida, Archosauromorpha, Crocopoda, Triassic, South Africa.

Gabriela Sobral [gabriela.sobral@smns-bw.de; ORCID: https://orcid.org/0000-0002-5001-4406], Staatliches Museum für Naturkunde Stuttgart, Rosenstein 1, 70191 Stuttgart, Germany.

Introduction

Prolacerta broomi Parrington, 1935, is a well-known stem-archosaur from the Lower Triassic of South Africa and Antarctica. The species was named by Parrington (1935) based on a small specimen (UCMZ 2003.41R) of an almost complete, partially disarticulated skull plus lower jaw (Fig. 1). Further specimens were subsequently described in the following decades by Camp (1945), Gow (1975), and Colbert (1987), whereas special attention was given to the braincase anatomy by Evans (1986). Meanwhile, Broom and Robinson (1948) described a new species, *Pricea longiceps*, which was later shown to represent a junior synonym of *Prolacerta broomi* by Gow (1975). More recently, Modesto and Sues (2004) presented new specimens from the Evolutionary Studies Institute (formerly, the Bernard Price Institute for Palaeontological Research) of the University of the Witwatersrand, offering a detailed review of the cranial anatomy in the known materials at the time. A new specimen from Antarctica was also described recently, providing new and detailed cranial information (Spiekman 2018). Currently, there are 13 recognised specimens from South Africa and Antarctica, and an unknown number of unassessed materials, including 16 from Antarctica (Colbert 1987; Ezcurra 2016; Spiekman 2018).

The importance of *Prolacerta broomi* for understanding the evolution of reptiles was recognised at the time of its discovery. When describing monospecific *Prolacerta*, Parrington (1935) noted a number of anatomical features that matched the hypothetical intermediate states proposed at the time, representing the evolution of lizards from "eosuchians" (a pre-cladistic, now paraphyletic stock of early diapsids, mainly represented by *Youngina* Broom, 1914). Despite this connection with lizards, Parrington (1935) nested *Prolacerta* not within lepidosaurs, but in its own family (Prolacertidae) within "Thecodontia", a group now largely represented by
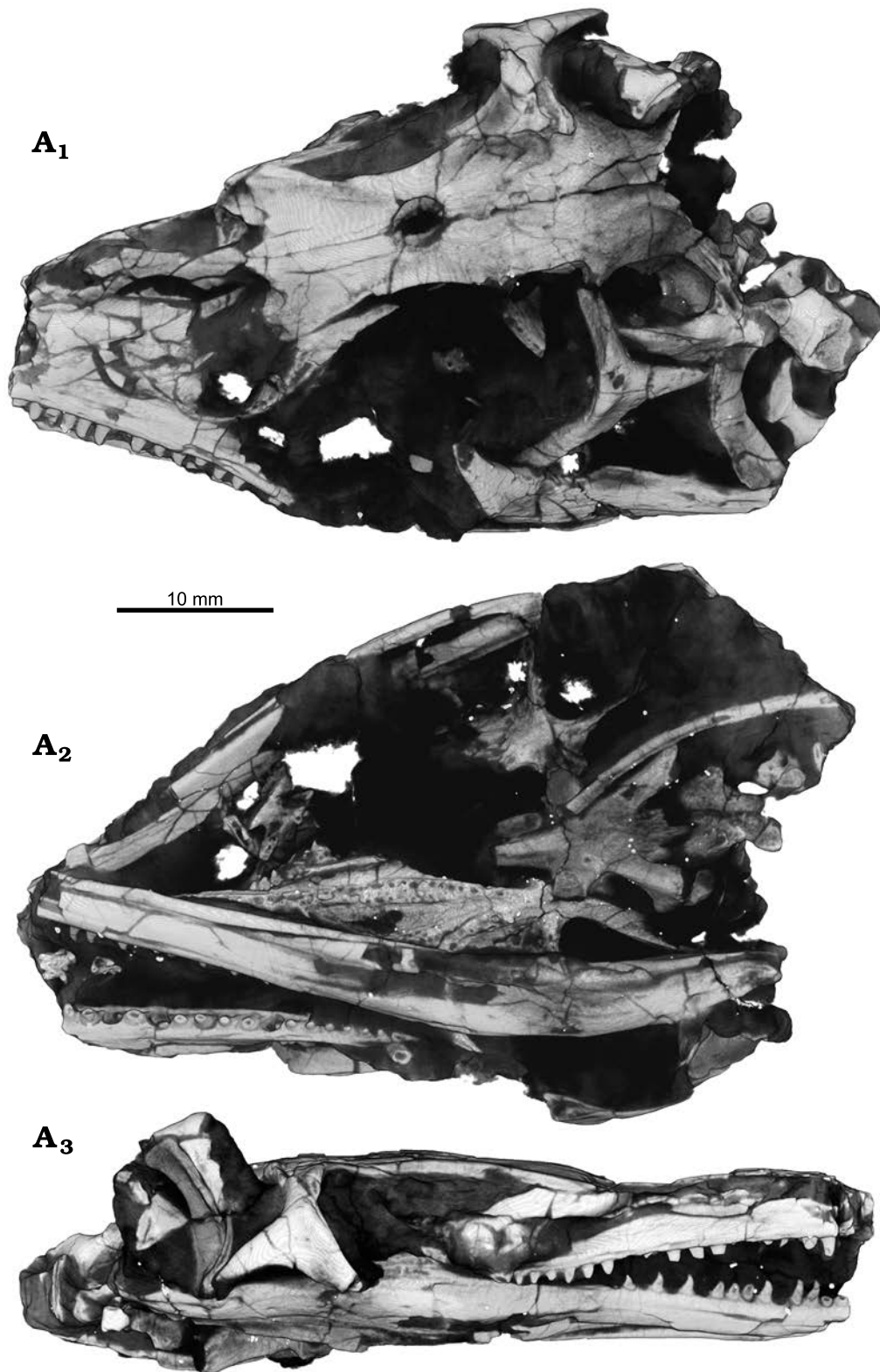
Fig. 1. Archosauromorph *Prolacerta broomi* Parrington, 1935, holotype UCMZ 2003.41R from Katberg Formation, *Lystrosaurus* Assemblage Zone, Karoo Basin; Induan, Lower Triassic; Harrismith Commonage, Free State, South Africa; rendered in 3D, in dorsal (A$_1$), ventral (A$_2$), and right lateral (A$_3$) views.

stem-archosaurs (non-archosaurian archosauromorphs). Soon after that, Camp (1945) argued that *Prolacerta*, together with *Protorosaurus*, should both be considered more closely related to lepidosaurs instead, and that "Eosuchia" should be replaced with the former "Protorosauria" of Huxley (1871). A heated debate on the classification of these two clades among reptiles, together with the most appropriate name for the group, followed in the next decades (Romer 1966;

Wild 1973; Brinkman 1981; Benton 1985; Chatterjee 1986; Evans 1988; Benton and Allen 1997; Rieppel et al. 2003), and the matter was not settled until more detailed work on the phylogenetic relationships of stem-archosaurs became available (Dilkes 1998; Müller 2004; Senter 2004; Nesbitt 2011; Ezcurra et al. 2014; Ezcurra 2016). The phylogenetic placement of *Prolacerta* in a family distinct from protorosaurians, and as an early-diverging archosauromorph closer to crown Archosuria than *Protorosaurus*, now has consensus (Nesbitt et al. 2015; Ezcurra 2016).

Holotypes are pivotal for taxonomy, as they define and name not only species, but also influence higher-level rankings. It is therefore vitally important to have the most detailed descriptions of type specimens. Despite the importance of *Prolacerta* in the evolutionary debates, and of the profusion of additional specimens, the holotype material of its type species (UCMZ 2003.41R) has never been described in detail. Here I revisit the original description and, with the aid of μCT techniques, provide new information on the cranial anatomy of the holotype of *Prolacerta broomi*.

Institutional abbreviations.—BPI, Evolutionary Studies Institute (formerly Bernard Price Institute for Palaeontological Research), University of Witwatersrand, Johannesburg, South Africa; UCMP, Berkeley Museum of Paleontology, University of California, Berkley, USA; UCMZ, University of Cambridge Museum of Zoology, Cambridge, UK.

Other abbreviations.—CN, cranial nerve; μCT, micro-computed-tomography; OTU, operational taxonomic unit.

Material and methods

The holotype UCMZ 2003.41R of *Prolacerta broomi* was scanned in the Museum für Naturkunde Berlin using a Phoenix|x-ray Nanotom (GE Sensing and Inspection Technologies GmbH, Wunstorf, Germany). X-ray slices were reconstructed in the software datos|x-reconstruction version 1.5.0.22 (GE Sensing and Inspection Technologies GmbH, Phoenix|x-ray). Scans comprised 1440 slices, and were made with a tungsten target using a 0.1 mm Cu filter with 110 KV, 90 μA, an exposure time of 500 ms, and a voxel size of 53.34 μm. The resulting volume was segmented and analyzed in VG Studio Max (Volume Graphics, Heidelberg, Germany). The CT data of this scan, together with the surface models of the segmented elements can be accessed on Morphosource through the address: https://www.morphosource.org/projects/000545071.

For the phylogenetic analyses, two data matrices were used as source data to add the holotype of *Prolacerta broomi* as an independent OTU and test its phylogenetic relationships: Ezcurra and Sues (2021) and Spiekman et al. (2021). For the latter dataset, the analysis with ratio characters included and specified characters ordered was the chosen one, with the a priori exclusion of the following taxa: *Macrocnemus*

obristi, Elessaurus gondwanoccidens. Tanytrachelos ahynis, Tanystropheus "conspicuus", and Raibliania calligarisi. Other parameters used for each search were the same as those specified in the corresponding studies.

Systematic palaeontology

Diapsida Osborn, 1903

Sauria Gauthier, 1984 sensu Gauthier et al. 1988

Archosauromorpha Huene, 1946 sensu Dilkes, 1998

Genus *Prolacerta* Parrington, 1935

Type species: *Prolacerta broomi* Parrington, 1935, see below; monotypic.

Prolacerta broomi Parrington, 1935

Figs. 1–16.

Holotype: UCMZ 2003.41R, an almost complete and dorsoventrally compressed skull with mandibles.

Type locality: Harrismith Commonage, Harrismith District, Free State, South Africa (Parrington 1935).

Type horizon: Katberg Formation, *Lystrosaurus* Assemblage Zone, Tarkastad Subgroup, Beaufort Group, Karoo Supergroup, Karoo Basin (Parrington 1935; Gow 1975; Modesto and Sues 2004). Induan, Lower Triassic (Groenewald and Kitching 1995).

Emended diagnosis.—*Prolacerta broomi* is an early diverging non-archosauriform archosauromorph distinguished from other saurians by the combination of the following characters: presence of the septomaxilla; maxilla with long horizontal dorsal margin and concave posterior margin; recurved maxillary teeth; parasphenoid ventral surface with two foramina for the carotid arteries located postero-medially to the basypterygoid processes; parasphenoid ventral surface with strong lateral crests; coronoid bone with marked postero-dorsal process and small postero-ventral process; tall splenial reaching up to the dental shelf for most of the mid-posterior medial surface of the lower jaw; splenial forming the ventral part of the mandibular ramus, with exposure in lateral view; extensive contact between the surangular and the prearticular in the articular region of the lower jaw; conical process on the proximal end of the humerus; ambiens process on the anterior margin of the pubis; ischial symphysis raised on a triangular shaped peduncle.

Remarks.—The current diagnosis proposed for *Prolacerta broomi* was given by Spiekman (2018). While some features listed therein could not be confirmed by the present study, one was found to be absent in UCMZ 2003.41R, namely the medially directed teeth on the pterygoid medial margin. The emended diagnosis provided above extends one character on the braincase and resurrects one character from Modesto and Sues (2004) and adds three new characters pertaining to the lower jaw. However, it does not exclude characters that could not be confirmed here, including the postcranial ones, because such broadscale evaluation is out of the scope of this work.
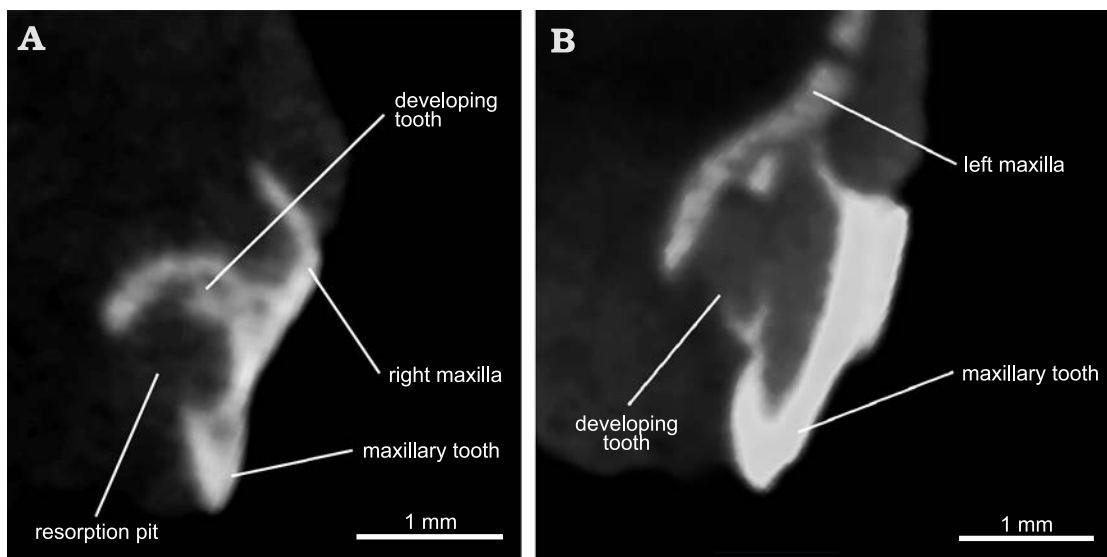
Fig. 2. Archosauromorph *Prolacerta broomi* Parrington, 1935, holotype UCMZ 2003.41R from Katberg Formation, *Lystrosaurus* Assemblage Zone, Karoo Basin; Induan, Lower Triassic; Harrismith Commonage, Free State, South Africa. Cross section through maxillary teeth showing resorption pits and replacement teeth. **A**. 13th preserved socket of the right maxilla. **B**. 1st preserved socket of the left maxilla.

Description.—The right maxilla has 17 alveoli and 12 teeth preserved. Of these, from anterior to posterior, the 3rd, 5th, and 10th sockets have small replacement teeth growing close to the labial side of the jaw. Additional, lingually located replacement teeth can be found in the 2nd, 4th, and 6th sockets. The teeth in the 8th, 13th and 16th sockets show resorption pits, the first one with no developing tooth but the latter two with very small tooth buds located labially in the pulp cavity (Fig. 2A). What appears to be the cross section of a tooth in ventral view of the material (Fig. 1A$_2$) is a hyoid element. The left maxilla (Fig. 3) has 15 sockets and 13 teeth. The teeth in the 7th, 12th, and 14th sockets are labial replacement teeth. Additionally, replacement teeth are found lingually in the 1st and 3rd sockets (Fig. 2B). These latter teeth, plus the ones in the 10th and 12th sockets, show resorption pits. A small tooth is found lingually between the 12th and 13th

sockets. The dorsal alveolar canal trends parallel to the tooth row and dorsal to the dental shelf. Posteriorly, the canal is open medially, forming a trough on the medial surface of the left maxilla. At the level of the 8th tooth socket, the canal enters the maxilla as the posterior alveolar foramen. It then trends within the maxilla all the way to its anteriormost preserved tip, giving off what appears to be a major lateral branch dorsal to the 6th socket (Fig. 3A$_1$). The foramen formed by this branch is much enlarged compared to the other foramina found on the lateral surface of the maxilla, but it is located too far posteriorly to be identified as the anterior alveolar foramen (anterior maxillary foramen, Modesto and Sues 2004), and its enlarged size is likely the result of post-mortem damage to a smaller nutrient foramen. On the medial surface of the dorsal process, there is a recess oriented antero-ventrally that corresponds to the medial
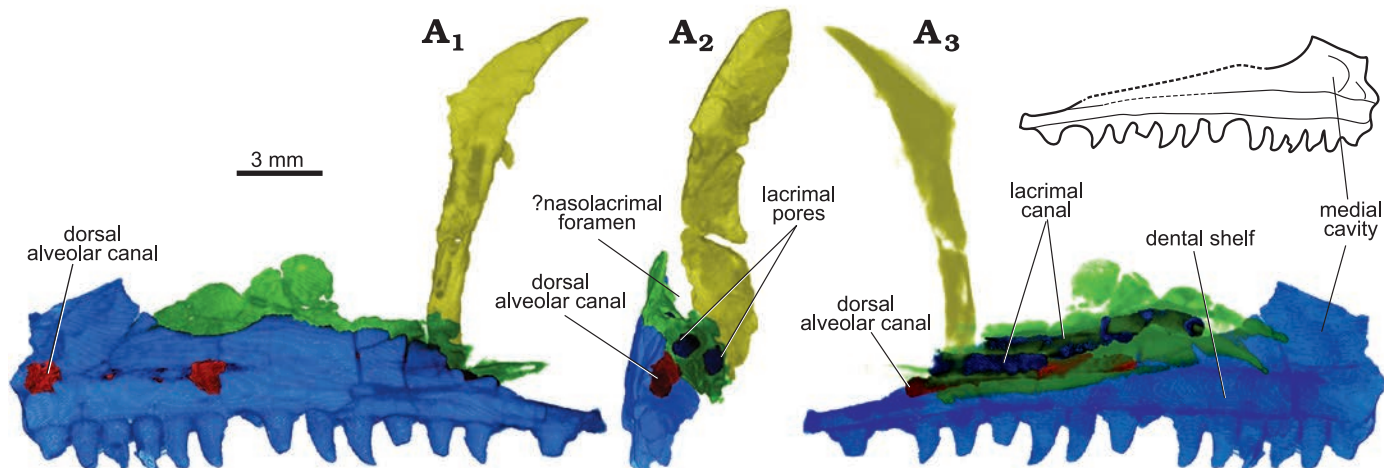

Fig. 3. Archosauromorph *Prolacerta broomi* Parrington, 1935, holotype UCMZ 2003.41R from Katberg Formation, *Lystrosaurus* Assemblage Zone, Karoo Basin; Induan, Lower Triassic; Harrismith Commonage, Free State, South Africa. Orbitonasal region, rendered in 3D, in left lateral (A$_1$), left medial (A$_2$), and posterior (A$_3$) views. Maxilla in blue, lacrimal in green, and prefrontal in yellow.

cavity of Ford and Benson (2018; maxillary sinus of Benoit et al. 2021). The recess is delimited anteriorly by a buttress that is only partially preserved.

Both nasals are present (Fig. 4A), but the left one is very closely associated with the left maxilla and it was very difficult to segment separately. The nasal is fragmented, but it would have been a fairly straight element on both lateral and medial borders. The posterior process diverges only slightly from the midline to border a small antero-medial extension of the frontals. Anteriorly, the lateral border of the nasal inflects laterally, making the bone broader here. As preserved, the entire anterior border of the nasal is mostly straight. Two subtle ridges (Fig. 4A$_2$) are found on the anterior border of the ventral surface, possibly representing the posteriormost portion of the nasal cavity.

Both lacrimals are present, but they are mostly concealed by the maxillae laterally. The left lacrimal (Figs. 3, 4B) is better preserved than the right one, which is badly crushed. The original identification of Parrington (1935) of the left lacrimal is incorrect. In his text-fig. 1, the lacrimal is identified as lying just ventral to the prefrontal, at the orbital rim. Segmentation of this element shows, however, that it corresponds to the ventral portion of the prefrontal. The lacrimal is an elongate bone whose anterior end is bifurcated and directed ventrally. A thin, rounded flange is present posterodorsal to the bifurcation, but its total extension cannot be defined. As preserved, the lateral surface of the lacrimal faces slightly ventrally, forming an opening in posterior view with the prefrontal, the nasolacrimal foramen (Fig. 3A$_3$; see Discussion). In dorsal view, the posterior half of the lacrimal is medially diverted, giving it a subtle sigmoid shape. The posterior half of the lacrimal formed the medial wall of the last section of the dorsal alveolar canal. The postero-ventral end of the lacrimal tapers to a small process, whose latero-dorsal margin bears a small thickened ridge that articulated with the dental shelf of the maxilla. Two canals are exposed in posterior view (Fig. 3A$_3$). The posterior end of the dorsalmost one is open laterally as well (Fig. 4B$_1$). The identifications of these structures are discussed below.

The prefrontals are preserved on both sides of the skull. The left prefrontal is preserved as a dorso-ventrally tall and thick element immediately bordering the anterior rim of the orbit (Figs. 3, 5A). A thin, short flange of bone extends anteriorly at its dorsal half, but it is incomplete. A canal trends dorsoventrally through the thickened orbital rim, but it is uncertain whether this is natural or the consequence of weathering. Nonetheless, a foramen is present ventrally on the medial surface of the prefrontal (Fig. 5A$_1$, in an area where the ventral nasal and the sphenopalatine arteries anastomose in *Iguania* (Porter and Witmer 2015). A similar canal is found in the prefrontal of the lepidosauromorph *Vellbergia* (Sobral et al. 2020). The right prefrontal (Fig. 5B) shows a complete posterior process, but the ventral one is damaged and missing its distalmost tip. The angle between the two is only slightly greater than 90°. Both processes are medio-laterally stout. In dorsal view, a shelf extends medio-
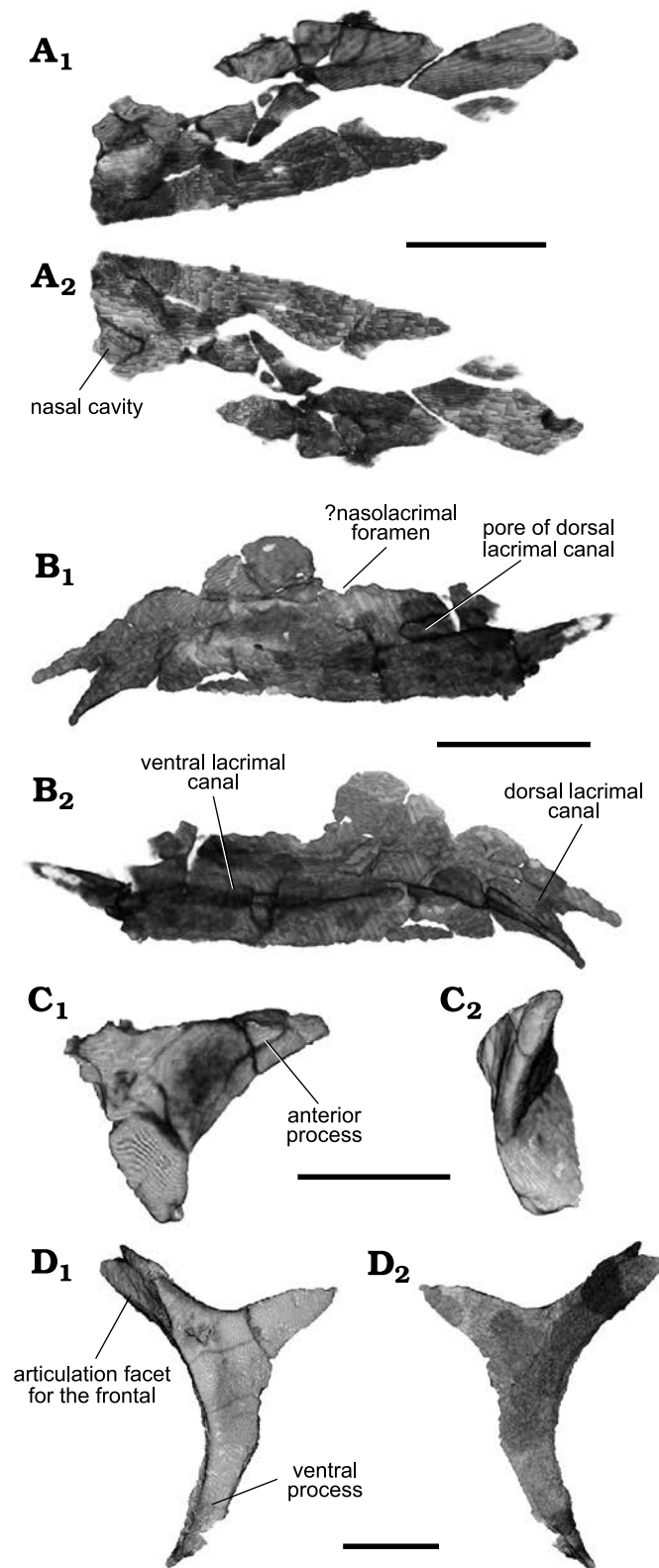

Fig. 4. Archosauromorph *Prolacerta broomi* Parrington, 1935, holotype UCMZ 2003.41R from Katberg Formation, *Lystrosaurus* Assemblage Zone, Karoo Basin; Induan, Lower Triassic; Harrismith Commonage, Free State, South Africa. Dermal bones of the skull, rendered in 3D: right nasal in dorsal (A$_1$) and ventral (A$_2$) views; left lacrimal in lateral (B$_1$) and medial (B$_2$) views; right postfrontal in lateral (C$_1$) and anterior (C$_2$) views; left postorbital in lateral (D$_1$) and medial (D$_2$) views. Scale bars 4 mm.
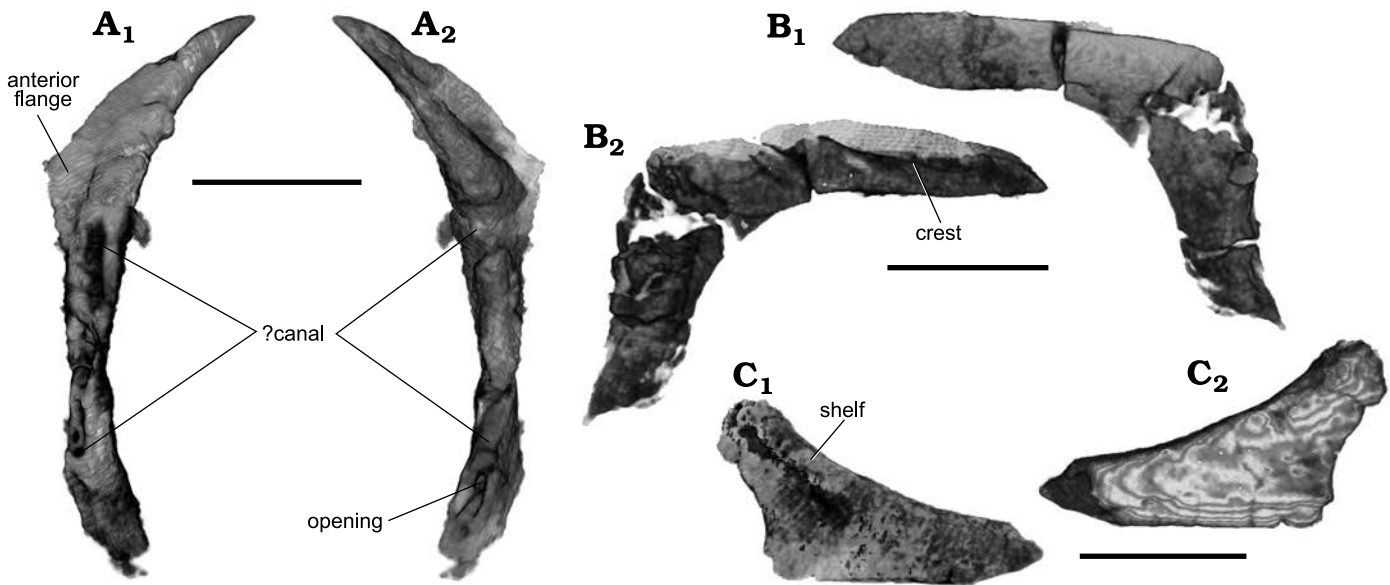
Fig. 5. Archosauromorph *Prolacerta broomi* Parrington, 1935, holotype UCMZ 2003.41R from Katberg Formation, *Lystrosaurus* Assemblage Zone, Karoo Basin; Induan, Lower Triassic; Harrismith Commonage, Free State, South Africa. Elements of the circumorbital region, rendered in 3D: left prefrontal in lateral (A_1) and medial (A_2) views; right prefrontal in medial (B_1) and lateral (B_2) views; fragment representing the main body of the left jugal in lateral (C_1) and medial (C_2) views. Scale bars 4 mm.

ally mid-length the posterior process (Fig. 5B_2). The right prefrontal does not show a thickened orbital rim with an internal canal, but the anterior flange is present and seems complete. It is short, not extending further anteriorly than the orbital margin.

The frontals (Figs. 1A_1, 6) are as described by Parrington (1935), although the drawing depicts a rather straight articulation with the nasals, whereas this is anteriorly concave. The frontal has a small leap of bone that underlies the nasals laterally (Fig. 6A_1). On the ventral surface, the crista cranii appears laterally at the level of the anteriormost extension of the postfrontal. The cristae are subtle and fade out at about the distalmost extension of the antero-lateral flange. It is difficult to follow the entire suture with the parietal, but the frontal appears to form the entire surface for articulation with the postfrontal (Fig. 6; see Discussion).

The postfrontal is absent on the left side. The right postfrontal is more boomerang-shaped than depicted by Parrington (1935), with the orbital rim being more concave (Figs. 4C, 6). The posterior process is more marked than originally illustrated, albeit still clearly shorter than the anterior and ventral ones. The postfrontal is bordered by the frontal and the postorbital, and there is no, or only a very limited contact with the parietal (see discussion).

The postorbital is markedly triradiate (Fig. 4D), with the ventral process being almost twice as long as the posterior process. The dorsal process is intermediate in size compared to the other two processes, and shows a deep embayment for the articulation with the postfrontal in its anterior surface (Fig. 4D_1). The postorbital is thickened medio-laterally at the orbital rim, but thinner posterior to it. A prominent elevation is present on the lateral surface of the bone ventral to the articulation with the postfrontal and

close to the orbital rim. It tapers as it trends ventrally along the orbital margin.

A portion of the left jugal is preserved (Fig. 5C). It is a triangular piece representing the main body of the bone. It is mostly hollow inside due to several channels trending within the base of the dorsal process, which eventually merge as a single opening in the anterior process. The angle formed by the preserved parts of these processes is slightly less than 160°. The posterior part of the bone seems intact, suggesting the absence of a posterior process. The medial surface is slightly concave, especially so at the main body and posterior half of the jugal, where the anterior border of the dorsal process forms a subtle shelf (Fig. 5C_2).

The parietals are mostly preserved, except for the distalmost portion of the postero-lateral process of the right side (Fig. 1A_1). The embayment that forms the dorsal part of the left upper temporal fenestra is well-marked. On the right side, however, no such structure can be seen, contrary to what is figured by Parrington (1935). Instead, the lateral surface of the right parietal curves smoothly ventrally. The quadrate has been dislodged in this region of the skull and its movement may have destroyed the embayment of the upper temporal fenestra. No parietal foramen was found.

No parts of the sclerotic rings were found, two palatal fragments are visible through the orbit on the left side.

Parrignton (1935) described the supratemporal as complete, but this is not the case. Two small parts are preserved on the left side close to the postero-lateral process of the parietal and to the posterior border of the squamosal.

Both squamosals are present, but the left is better preserved than the right one (Fig. 7A). The right squamosal is present as a thin cap on the top of the quadrate, together with part of its ventral process (Fig. 7B). As preserved, the
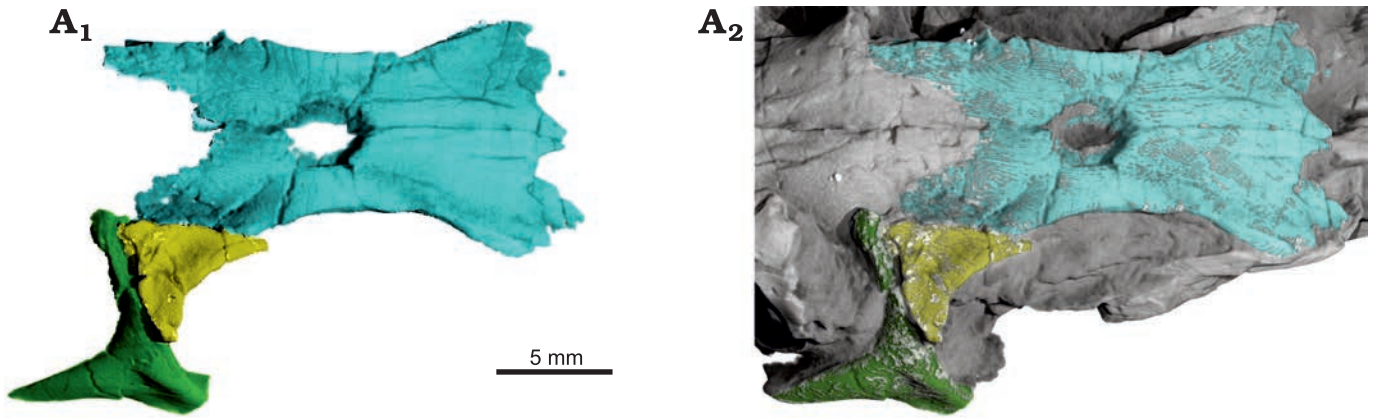
Fig. 6. Archosauromorph *Prolacerta broomi* Parrington, 1935, holotype UCMZ 2003.41R from Katberg Formation, *Lystrosaurus* Assemblage Zone, Karoo Basin; Induan, Lower Triassic; Harrismith Commonage, Free State, South Africa. Articulation between frontals (blue), right postfrontal (yellow), and right postorbital (green) in dorsal view. Segmented bones as 3D renderings alone (A$_1$) and juxtaposed with the remaining of the skull (A$_2$). Anterior to the right.
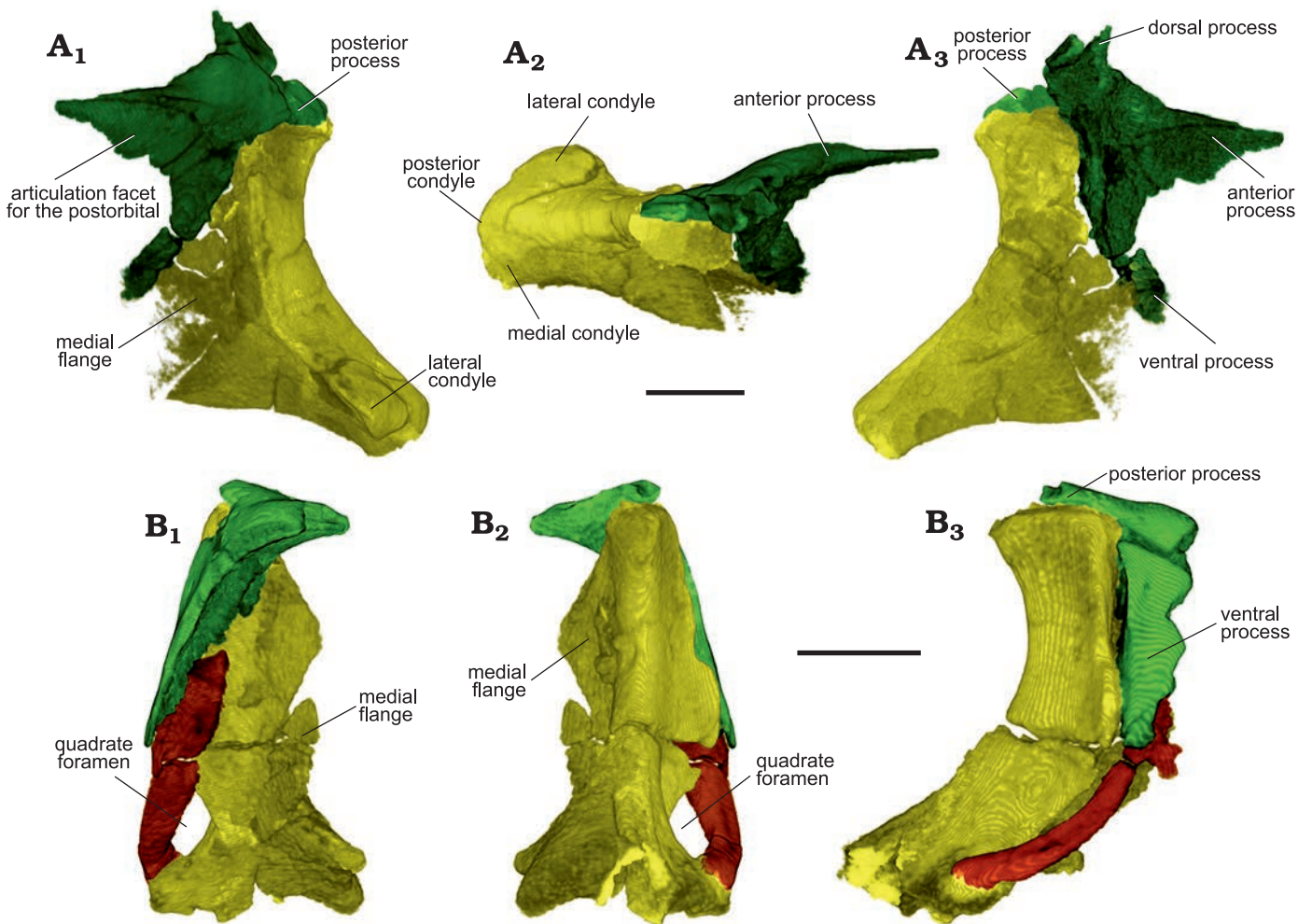

Fig. 7. Archosauromorph *Prolacerta broomi* Parrington, 1935, holotype UCMZ 2003.41R from Katberg Formation, *Lystrosaurus* Assemblage Zone, Karoo Basin; Induan, Lower Triassic; Harrismith Commonage, Free State, South Africa. Suspensorium showing the quadrate (yellow), squamosal (green), and quadratojugal (brown). Rendered in 3D. Right side in lateral (A$_1$), dorsal (A$_2$), and medial (A$_3$) views; left side in anterior (B$_1$), posterior (B$_2$), and lateral (B$_3$) views. Scale bars 3 mm.

anterior process is a single projection. Two marked ridges trend along the posterodorsal region of the lateral surface of the squamosal in a V shape, with the opening directed anteriorly. These ridges delimit the articulation surface with the postorbital (Fig. 7A$_1$). The flange of bone between the ridges is extensive, indicating a good overlap between postorbital and squamosal. The ventral process extends ventrally until about the mid-height of the quadrate. The medial side of the

squamosal is marked by a strong U-shaped ridge facing anteriorly. The surface within this ridge is concave. The short posterior process overlies the head of the quadrate. There is also a small dorsomedial process for the contact with the supratemporal. The main body of the squamosal is broad and medially concave, forming part of the upper temporal fenestra.

The quadrate is preserved almost completely on both sides (Fig. 7). The dorsal quadrate head is flat and antero-posteriorly elongate in dorsal view (Fig. 7A$_3$). In lateral view, the quadrate is strongly curved posteriorly. The posterior border of the quadrate forms a thick dorso-ventral ridge that separates the lateral and medial sides of the bone. The lateral flange of the quadrate is antero-posteriorly short when compared, for instance, with *Mesosuchus* (Sobral and Müller 2019), and its anterior border is delimited by a strong crest. The quadrate does not sheath the squamosal posteriorly (Fig. 7B$_2$). The medial flange is incomplete on both sides, due to preservation. The surface between this flange and the posterior ridge is much less concave than the surface between the ridge and the lateral flange. The anterior surface of the quadrate between the medial and lateral flanges is also smoothly concave. The angle formed between the two flanges is about 60°. The ventral quadrate head is divided in three condyles areas: a lateral, a posterior, and a medial one (Fig. 7A$_3$). The lateral condyle is the more well-developed of the three. The medial and posterior condyles lie in the same plane, whereas the lateral one is positioned more anteriorly, and slightly ventrally, in relation to the other two. The medial condyle smoothly connects with the medial flange.

The quadratojugal is present on the right side (Fig. 7B). It is a thin and long rod of bone articulating with both the anterior surface of the quadrate ventrally and the ventral process of the squamosal dorsally. On the ventral half of its lateral surface, there is a longitudinal ridge parallel and close to the anterior border, behind which the surface is slightly depressed. The quadratojugal is posteriorly concave, following the curvature of the quadrate in lateral view, but also medially concave in its ventral half when seen posteriorly, forming a foramen together with the quadrate in posterior view. The quadratojugal has no anterior process.

The palate is crushed and it was very difficult to digitally segment out the elements individually (Fig. 8). Contrary to Parrington (1935), however, it was not possible to identify the septomaxilla confidently. There are several hyoid elements preserved, some of which are visible externally in the material (Fig. 1A$_2$).

The right pterygoid is almost completely preserved, but the left one is represented by its posterior portion only. In ventral view, most of the pterygoid is seen externally (Fig. 1A$_2$), but the anterior or palatal ramus continues some extent anteriorly within the matrix and is concealed by the right lower jaw. The medial border of the pterygoid is almost straight (Figs. 1A$_2$, 8), except for its mid-length, which is slightly convex medially, and the posterior third, where it is slightly concave medially, similar to the palate
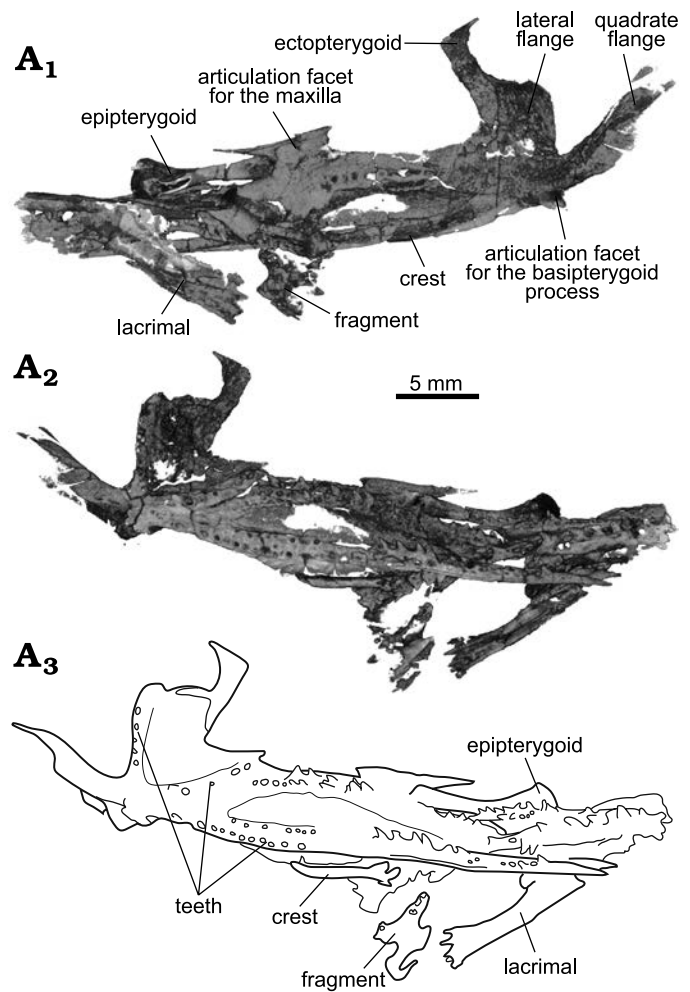

Fig. 8. Archosauromorph *Prolacerta broomi* Parrington, 1935, holotype UCMZ 2003.41R from Katberg Formation, *Lystrosaurus* Assemblage Zone, Karoo Basin; Induan, Lower Triassic; Harrismith Commonage, Free State, South Africa. Palate, rendered in 3D, in dorsal (A$_1$) and ventral (A$_2$) views; line drawing of the palatal ventral surface (A$_3$).

reconstruction of Gow (1975). The medial rim of the palatal ramus has two parallel lines of teeth, the medialmost of which shows smaller teeth and reaches farther posteriorly. The teeth on the lateral line are recurved posteriorly. On the mid-third of the pterygoid, medial to the tooth row, a worn-out portion of a raised crest is preserved (Fig. 8A$_2$), lacking alveoli or any other sign of teeth. This crest on the pterygoid resembles the one present in the palate of *Taytalura* (Martinez et al. 2021: fig. S3), albeit much less dorsally developed in UCMZ 2003.41R. The lateral border of the pterygoid trends smoothly from the lateral flange antero-laterally up to the palatine articulation with the maxilla (Fig. 8A$_1$), forming the rounded medial border of the suborbital fenestra, but it is not possible to discern the suture between both bones. The lateral border of the palatine trends almost straight anteriorly on the ovoid posteromedial border of the choana, but it is soon lost amid other fragments of the palate. Another row of teeth trends along the lateral border of the pterygoid and onto the palatine until the point
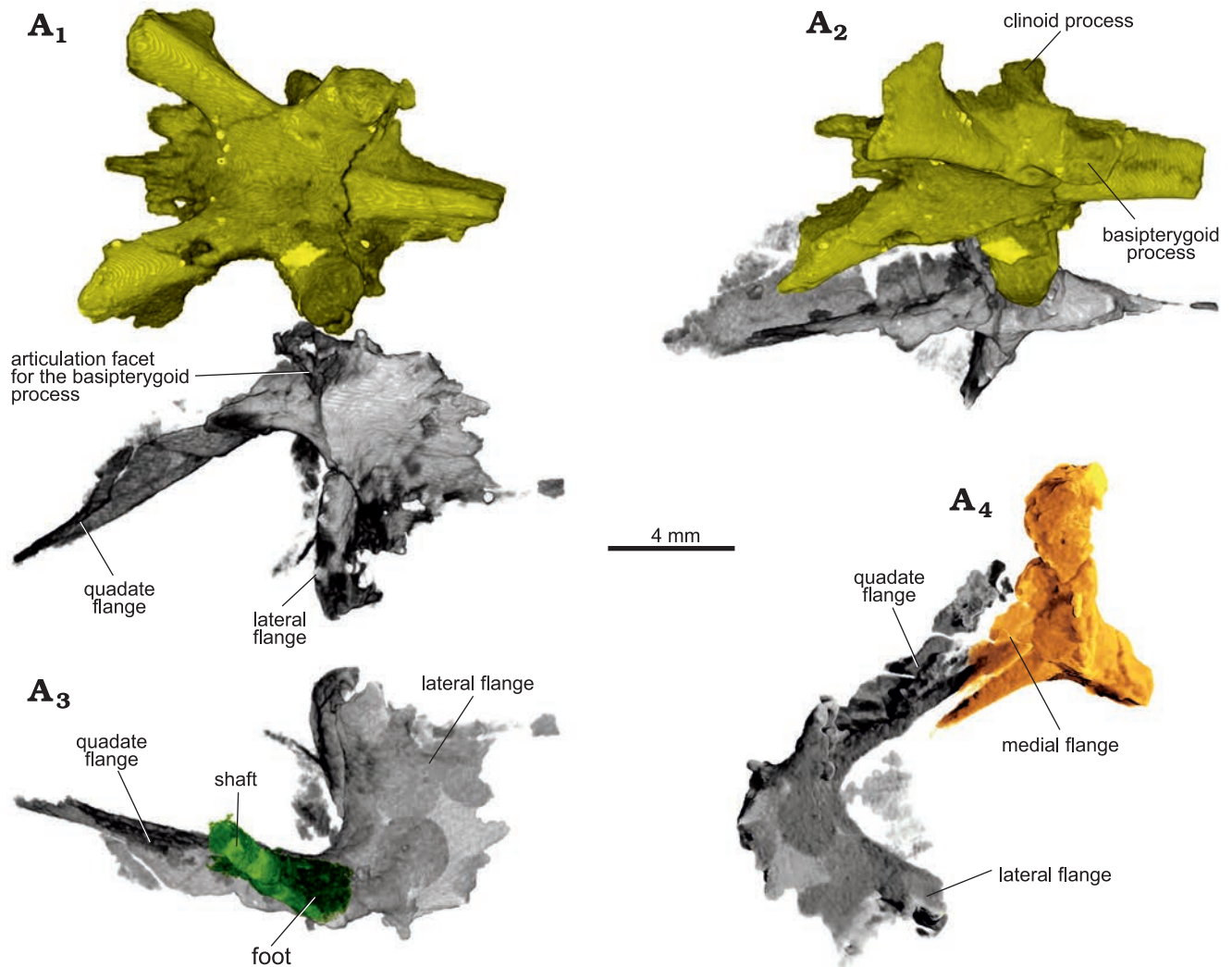
Fig. 9. Archosauromorph *Prolacerta broomi* Parrington, 1935, holotype UCMZ 2003.41R from Katberg Formation, *Lystrosaurus* Assemblage Zone, Karoo Basin; Induan, Lower Triassic; Harrismith Commonage, Free State, South Africa. Craniopalatal articulation, rendered in 3D, showing the left pterygoid (gray), parabasisphenoid (yellow), left epipterygoid (green), and left quadrate (orange) in ventral (A_1), ventromedial (A_2), and dorsal (A_3) views, and antero-dorsal view of the left side (A_4).

where the palatine disappears among the fragments. These fragments include two or three long strips of tooth-bearing bone, which indicates that this second, lateral row of teeth continued onto the vomer. This row shows two lines of well-developed but blunt teeth on the pterygoid and more anteriorly on the vomer, but not in the palatine region. The vomer also shows a medial row of well-developed teeth. The palatal surface of the lateral flange of the pterygoid is broad and rounded (Figs. $8A_1$, $9A_3$), and its ventral surface in this area is smoothly concave. The posterior part of the flange curves ventrally, but does not extend much beyond the level of the palate. A single row of teeth trends along the rim of the posterior margin, which is slightly anteromedially to lateroposteriorly directed. In medial view, the articulation socket for the basipterygoid process of the basisphenoid (Figs. $8A_1$, $9A_1$) is shallow and ovoid, with the long axis oriented anteroposteriorly (Fig. $9A_1$, A_2). As preserved, the medial surface of the quadrate flange is

strongly concave (Figs. $8A_1$, 9). It reaches up to the dorsal third of the quadrate bone (Fig. $9A_4$).

The right ectopterygoid (Fig. 8) is completely preserved and in articulation with the lateral flange of pterygoid, whereas the left one is also complete and associated with the left pterygoid, but not articulated (Fig. 10A). The general shape of the ectopterygoid is that of a "Y" in dorsal and ventral views. The anterior border is almost straight, whereas the posterior border is concave posteriorly. Laterally, the ectopterygoid is posteriorly expanded as a small foot for the contact with the jugal. Medially, the ventral surface of the ectopterygoid is concave for the articulation with the lateral flange of the pterygoid, whereas the stem of the "Y" is rod-like in cross section. In dorsal view, a subtle ridge trends from the posteriorly directed foot to the base of the bifurcation proximally.

The right epipterygoid is complete (Figs. 8, 10B). It is much displaced anteriorly, being found anterior to the orbit.
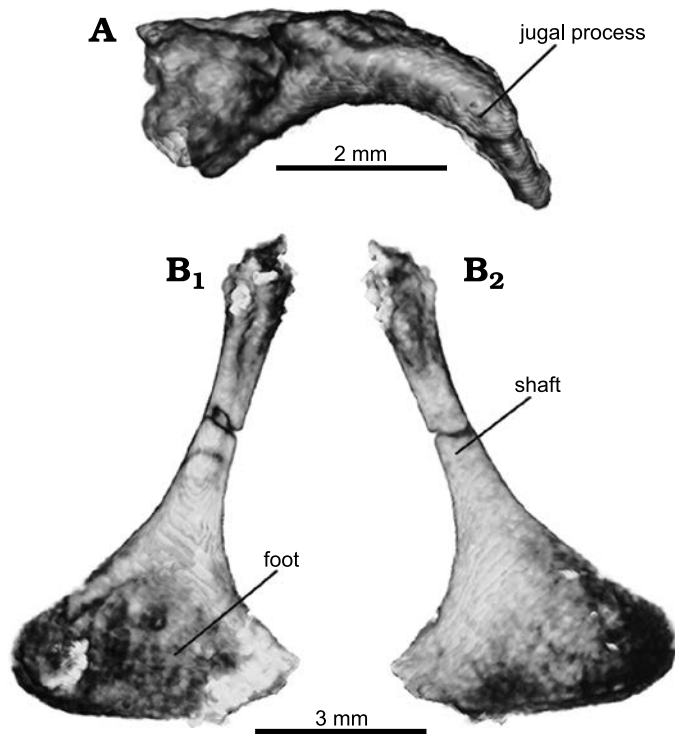
The epipterygoid has a broad and medially concave footplate. The angle between the rod and the footplate is acute, so that, in anatomical articulation, the anterior tip of the footplate lies well anterior to the shaft. The anterior portion of the footplate is shorter than the posterior one. The shaft has a small dorsal head, whose tip is expanded laterally in anterior view. A subtle ridge trends dorso-ventrally on the postero-medial surface of the shaft. The left epipterygoid is much less complete, but preserved in articulation with the left pterygoid (Fig. 9A$_3$).

The braincase is present in its entirety, but for a good part, not well-preserved. The braincase floor is externally visible on the ventral surface of the material (Fig. 1A$_2$). The elements of the braincase floor are disarticulated, not fused, in contrast to what was described by Parrington (1935). The parabasisphenoid is missing most of the cultriform process (Figs. 9, 11). The foramina for the internal carotid arteries

Fig. 10. Archosauromorph *Prolacerta broomi* Parrington, 1935, holotype UCMZ 2003.41R from Katberg Formation, *Lystrosaurus* Assemblage Zone, Karoo Basin; Induan, Lower Triassic; Harrismith Commonage, Free State, South Africa. Isolated palatal elements, rendered in 3D: **A**. Left ectopterygoid in ventral view. **B**. Right epipterygoid in medial (B$_1$) and lateral (B$_2$) views.

Fig. 11. Archosauromorph *Prolacerta broomi* Parrington, 1935, holotype UCMZ 2003.41R from Katberg Formation, *Lystrosaurus* Assemblage Zone, Karoo Basin; Induan, Lower Triassic; Harrismith Commonage, Free State, South Africa. Braincase floor, rendered in 3D showing the parabasisphenoid (yellow) and basioccipital (blue) in association in dorsal (A$_1$), ventral (A$_2$), left lateral (A$_3$), and posterior (A$_4$) views. Anterior to the top in A$_1$, A$_2$.

are located medio-posteriorly to the basipterygoid processes in ventral view (Fig. 11A$_2$). They trend medially and anteriorly within the parabasisphenoid, and open dorsally as separate foramina in a common fossa (Fig. 11A$_1$). The basipterygoid processes are squared and lateroventrally directed. The articulation facet for the pterygoid are found distally (Figs. 9A$_1$, A$_2$, 11A$_2$). On the dorsal surface of the bone, the dorsum sellae are low and there is no sign of the course of the abducens nerve (CN VI). The clinoid process is present on the right side only. The basioccipital is displaced posteriorly. The basioccipital contribution to the basal tuber is intact on the left side, whereas on the right the distalmost portion is absent. The tubera are small, and extend ventrally and posteriorly (Fig. 11A$_3$). A semilunar depression was not found on either side, but the left parabasisphenoid contribution to the basal tubera bears a low crest trending proximodistally parallel very close to its ventral border. Dorsal to it, the lateral surface of the tuber is smoothly concave on both sides as seen in posterior view (Fig. 11A$_4$). The area is not well-preserved on the left side, so that confirming the crest and the concavity as the semilunar depression is not possible. On the right side a crest is absent. The occipital condyle is damaged. As preserved, the basioccipital contributed less than half of the length of the braincase floor.

The remaining of the braincase is disarticulated within the matrix. The supraoccipitals form one piece that is flat dorsally and exhibit two projections ventrally that form the dorsal portion of the otic capsule. The left prootic is better preserved, so the description will mostly be based on it (Fig. 12). The alar crest is found dorsal to the round foramen for the trigeminal nerve (CN V). The anterior inferior process of the prootic are damaged on both sides, being mostly absent on the left side and incomplete on the right. It formed the ventral border of the trigeminal foramen. There is a fossa for the gasserian ganglion on the posterodorsal border of the foramen, anterior to the otosphenoidal crest. The foramen for the facial nerve (CN VII) is located posterior to the crest (Fig. 12B). The prootic is quite medio-laterally thin in this region. The anterior portion of the vestibule is located dorsal and posterior to the foramen of CN V, occupying the main body of the bone (Fig. 12A$_3$). In medial view, the floc-
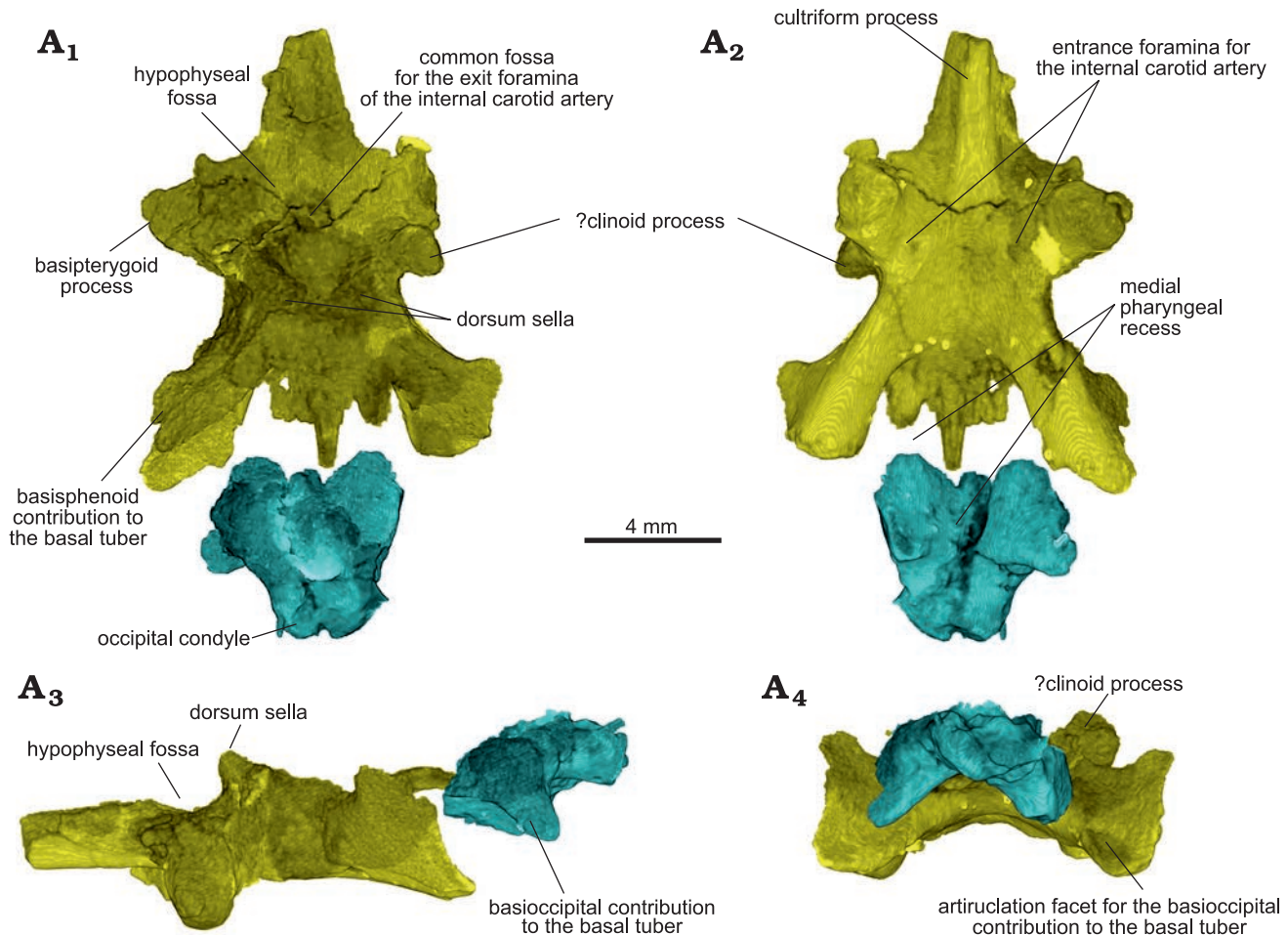

Fig. 12. Archosauromorph *Prolacerta broomi* Parrington, 1935, holotype UCMZ 2003.41R from Katberg Formation, *Lystrosaurus* Assemblage Zone, Karoo Basin; Induan, Lower Triassic; Harrismith Commonage, Free State, South Africa. Prootics, rendered in 3D: **A**. Left element in lateral (A$_1$), medial (A$_2$), and posterior (A$_3$, A$_4$) views. **B**. Right element in lateral view. Roman numerals refer to corresponding cranial nerves.

cular recess is somewhat antero-posteriorly elongate. The vestibule bulges into the cranial cavity, forming a partially open medial wall. Antero-ventral to the vestibule, a round mark could indicate the position of the anterior branch of the vestibulo-cochlear, or auditory, nerve (CN VIII).
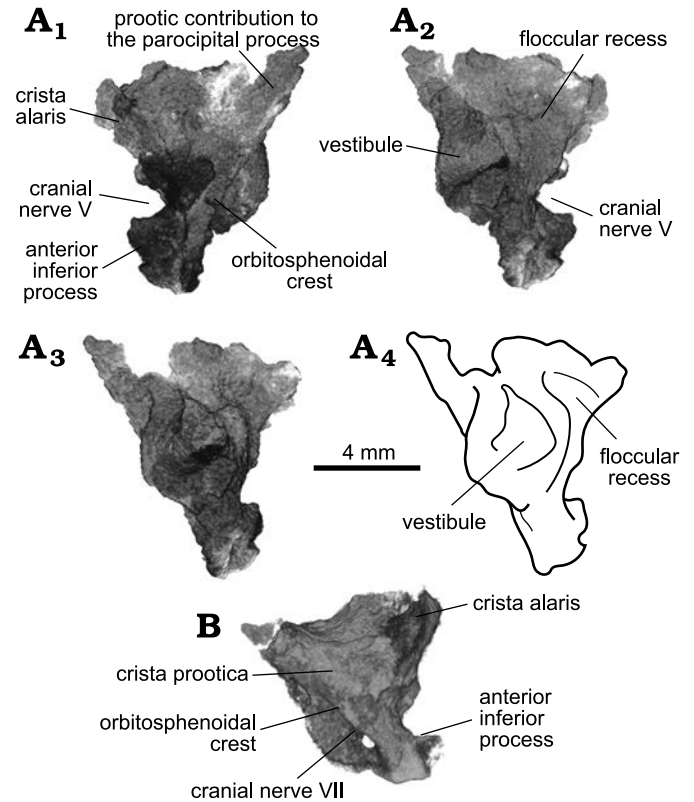
The left opisthotic is displaced to the right side and severely damaged, whereas the right one is crushed and distorted (Fig. 13A). Except for the posterior portion of the vestibular recess, not many features are visible. The ventral ramus shows no medial expansion delimiting the otic cap-

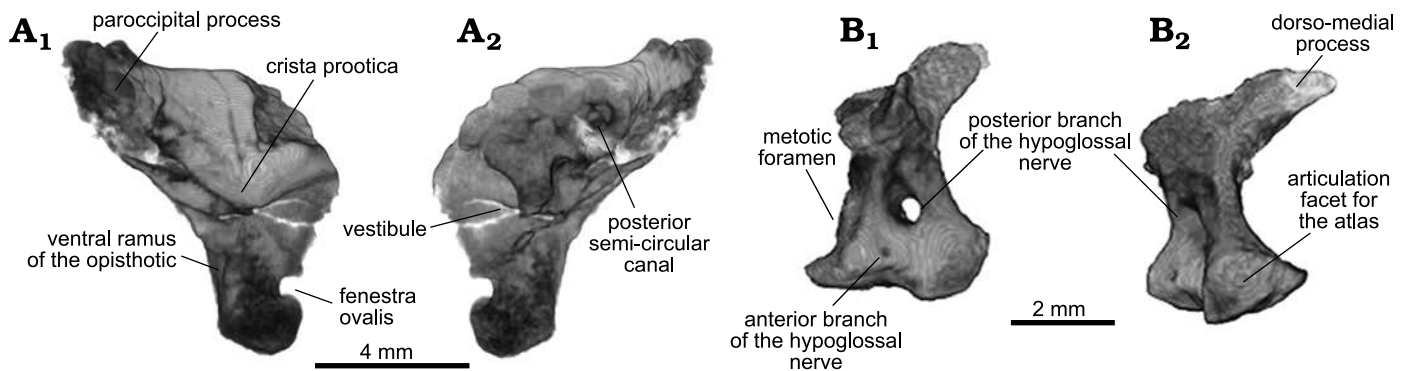

Fig. 13. Archosauromorph *Prolacerta broomi* Parrington, 1935, holotype UCMZ 2003.41R from Katberg Formation, *Lystrosaurus* Assemblage Zone, Karoo Basin; Induan, Lower Triassic; Harrismith Commonage, Free State, South Africa. Other braincase elements, rendered in 3D: right opisthotic in lateral (A$_1$) and medial (A$_2$) views; left exoccipital in lateral (B$_1$) and posterior (B$_2$) views.

sule ventro-posteriorly (Fig. 13A$_2$), as in BPI 2675 (Evans 1986). The fenestra ovalis shows a morphology that resembles that of *Mesosuchus* (Sobral and Müller 2019), in which it is formed by a recess with a smaller, more medial opening inside of it. Finally, both exoccipitals are present and well preserved. On the left side, the foramen for the posterior and main branch of the hypoglossal nerve (CN XII) is clearly visible, whereas a very small hole is found ventral and slightly anterior to it, for the anterior ramus (Fig. 13A$_1$). They are also present on the right side, albeit obliterated and less clearly visible. The postero-ventral portion of the exoccipital is expanded, stout, and rounded, indicating it could have taken part in the occipital condyle, but currently it is difficult to confirm. The exoccipital has a well-developed dorsomedial process that would make most of the rim of the foramen magnum (Fig. 13A$_2$). It is not possible to know if the contralateral exoccipitals met dorsally or ventrally.

The supraoccipitals are complete but not well preserved (Fig. 14A). The bones are tightly sutured together, being impossible to follow their contact in the CT scans. As preserved, the dorsal surface is broad and flat with no distinct features. In this view, the posterior border is narrower than the anterior one, giving it an anteriorly flaring outline. The anterior rim is convex anteriorly while the posterior one is concave. The ventral surface bears two antero-posteriorly elongate projections, parallel to each other and lying close to their corresponding lateral borders. These projections house the dorsal part of the inner ear (part of the anterior and posterior semicircular canals and the common crus) and likely contacted the opisthotic and prootic, delimiting the posterior region of the endocranial cavity dorsolaterally. The supraoccipitals formed the dorsal portion of the foramen magnum.

Given the poor preservation of the braincase, the segmentation of the inner ear is incomplete on both sides, especially on the left side. However, different parts were preserved so that a general picture can be given (Fig. 14B). There are two bony ampullae anteriorly for the anterior and lateral semicircular canals each, which are located rather dorsally in the vestibule. The ampulla of the lateral semicircular canal is positioned posteriorly and dorsal to the ampulla for the anterior canal. The anterior canal arches broadly postero-medially. The lateral canal, in contrast, does not trend too far away from the vestibule. The posterior semicircular canal first leaves the vestibule in a dorsomedial direction, arching more strongly anteriorly only at mid-length, to reach the common crus. This first medial direction of the posterior semicurcular canal contrasts to the condition of other diapsids and archosauromorphs, such as *Elachistosuchus* (Sobral et al. 2015), *Mesosuchus* (Sobral and Müller 2019), or *Euparkeria* (Sobral et al. 2016). In these, the posterior canal first trends laterally, before turning antero-medially into the common crus.

Both lower jaws are quite damaged, with some elements in tight articulation in some places (Fig. 15). The articular is only present on the left side. It is Y-shaped in coronal view and CT scans show it is formed of trabecular bone, in con-

Fig. 14. Archosauromorph *Prolacerta broomi* Parrington, 1935, holotype UCMZ 2003.41R from Katberg Formation, *Lystrosaurus* Assemblage Zone, Karoo Basin; Induan, Lower Triassic; Harrismith Commonage, Free State, South Africa. Partial skull roof and inner ear, rendered in 3D: **A**. Supraoccipitals in posterodorsal (A$_1$) and posterior (A$_1$) views; **B**. Right inner ear in lateral view. Please note that the different parts of the inner ear in B represent segmentations from elements of the braincase that are in disarticulation (prootic, opisthotic, supraoccipitals); they are shown here close to one another for illustration purposes only and may therefore not represent the real dimensions of this structure with precision.

trast to the other lower jaw elements. The dorsal surface of the articular has a shallow groove, and the medial arm of the Y is more developed than the lateral one. The articular was completely sheathed by the surangular laterally and by the prearticular medially.

The prearticular covered the articular medially. Its dorsal rim is raised and slightly concave posteriorly, so that the
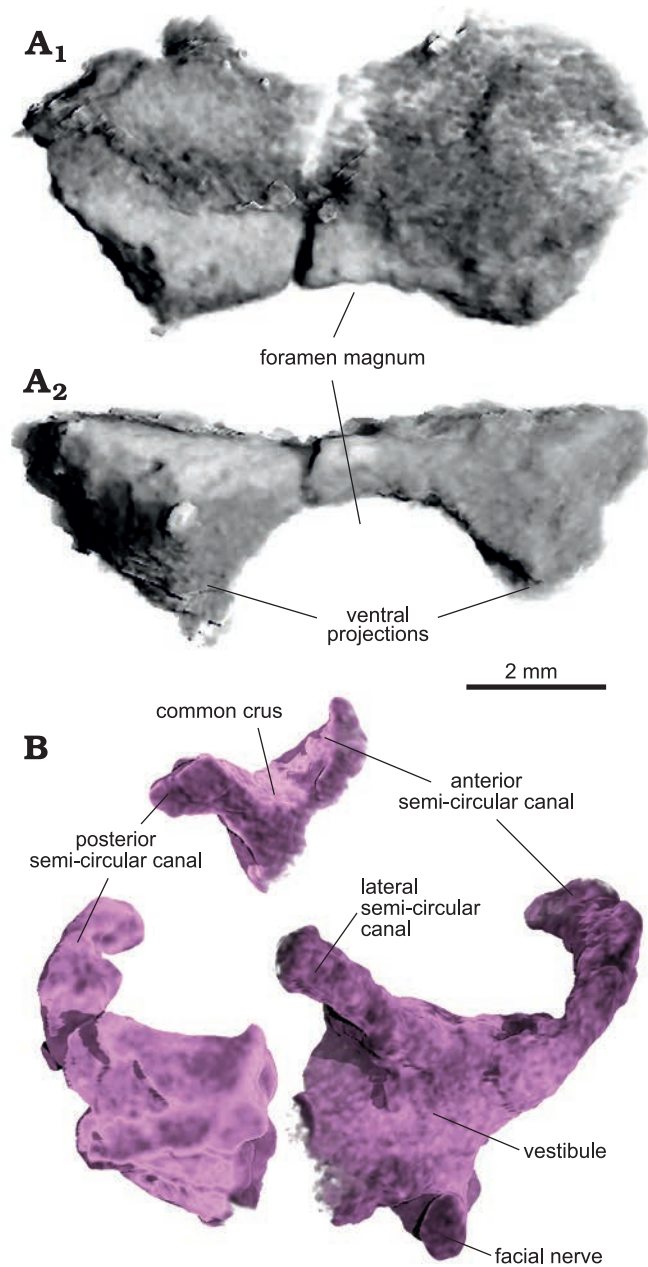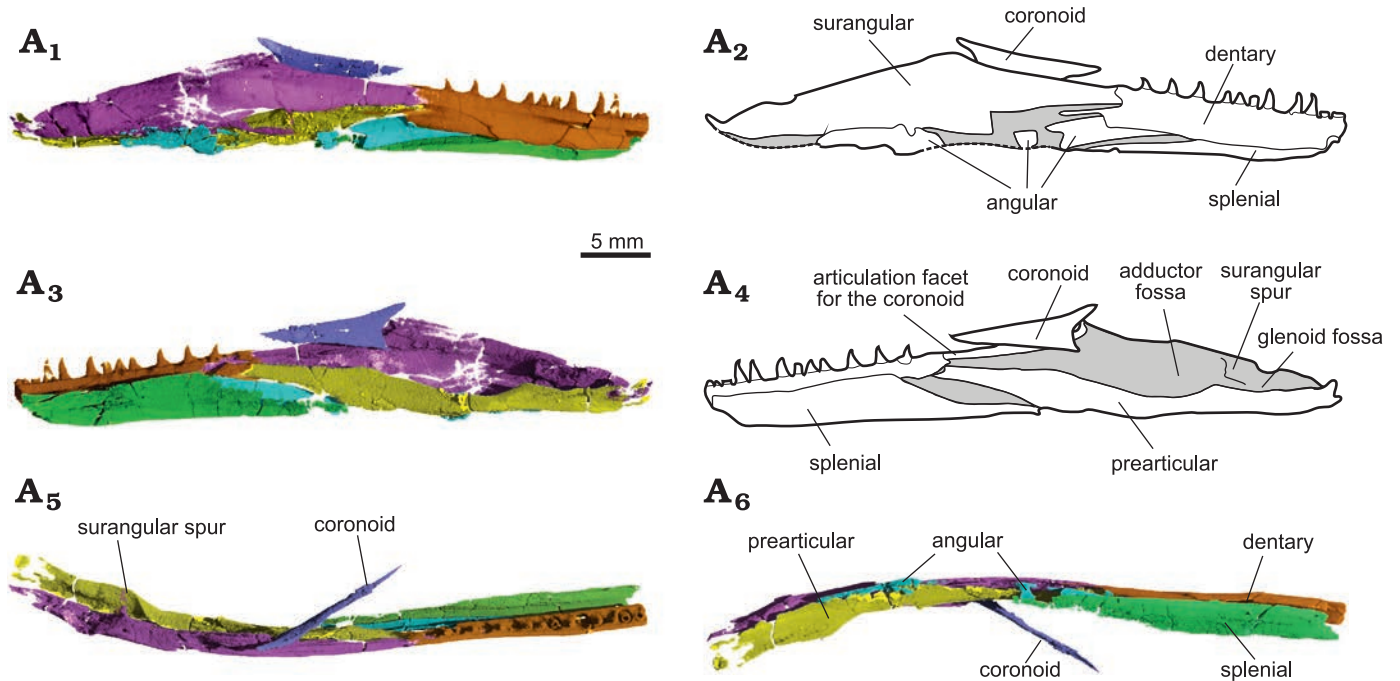
Fig. 15. Archosauromorph *Prolacerta broomi* Parrington, 1935, holotype UCMZ 2003.41R from Katberg Formation, *Lystrosaurus* Assemblage Zone, Karoo Basin; Induan, Lower Triassic; Harrismith Commonage, Free State, South Africa. Right ramus of the lower jaw in lateral (A_1, A_2), medial (A_3, A_4), dorsal (A_5), and ventral (A_6) views, showing the surangular (pink), dentary (orange), angular (blue), splenial (green), prearctular (yellow), and coronoid (purple).

glenoid fossa is directed mostly dorsally (Fig. 14A_2). More anteriorly, the concavity deepens abruptly to form the large and medially open adductor fossa. The prearticular does not reach further anteriorly than the last dentary tooth. Even though the prearticular and surangular are not in contact, they probably did at the posteriormost region of the lower jaw, because the medial borders of both bones complement one another ventrally (Fig. 15A_6).

The angular is very long, reaching up to the 5th tooth socket anteriorly, but it is mostly concealed within the mandibular ramus. It does not participate in the retroarticular process, reaching the level of the surangular spur posteriorly, between the glenoid and adductor fossae. The angular is exposed laterally on the lateral surface of the lower jaw in this region, but because the jaw is damaged here, the total anterior extent of this lateral exposure is impossible to determine. The angular eventually turns medially and trends within the mandibular ramus.

The surangular forms most of the lateral surface of the posterior portion of the lower jaw, limiting the angular to the ventral region and likely covering the articular laterally. A subtle shelf gives the bone a laterally convex outline in posterior or anterior views. The surangular forms the coronoid eminence almost entirely, and a good portion of the dorsal rim of the jaw anterior to it as well. A small anterior surangular foramen is present immediately ventral and posterior to the contact with the coronoid bone. It runs anterolaterally to posteromedially within the surangular, where it is joined by another channel ventrally, to open on the floor of a main canal trending within the bone. Likewise, a posterior surangular foramen is found close to the surangular dorsal border,

anterior to its articulation with the quadrate and posterior to the level of the medial spur. It immediately opens into another main canal within the bone. The surangular spur is prominent but thin, and separates the glenoid from the adductor fossae (Fig. 15A_3, A_5). The coronoid bone is preserved almost in place. It is a thin split of bone restricted to the lingual side of the jaw. Its articulation facet for the coronoid lies entirely on the surangular (Fig. 15A_3).

The splenial is poorly preserved at its posterior end and missing its anterior portion. It is a tall element, reaching up to the dental shelf dorsally. It formed the entire medial surface of the jaw and the entire floor of the mandibular ramus in this region (Fig. 15A_6). Except for its posterior third, the splenial bears a well-developed canal trending antero-posteriorly through the ventral end of the mandibular ramus. Along its course, it is joined by several smaller canaliculi that seem to open mostly on the lateral surface of the bone and into the Meckelian canal. A tiny opening at the posterior part of the splenial seems to run medio-laterally. It is, however, very difficult to reconstruct them because of the several breaks on the bone.

As it stands, the dentary is mostly restricted to a more dorsal position in the mid-posterior region of the lower jaw, allowing a small participation of the splenial in the mandibular ramus in lateral view (Fig. 15A_1). There is also no clear articulation facet on the surangular indicating that the dentary could reach as far posteriorly as the coronoid eminence dorsally, although its posterior extent must have been farther than the last dentary tooth, as indicated by a splint of bone on its lateral mid-height (Fig. 15A_1). The left dentary has 17 alveoli and 13 teeth preserved, plus a partial tooth

anterior to the anteriormost tip of the dentary. The teeth in the 6th, 9th, and 12th sockets are new replacement teeth growing on the labial side of the jaw. The tooth in the 4th socket shows a resorption pit and a very small replacement tooth on the labial side. The tooth in the 15th socket may show a resorption pit as well, but because there is damage here, it is difficult to confirm. The right dentary has 11 teeth preserved in 16 alveoli, with small erupting teeth in the 5th, 12th, 14th, and 16th sockets. The teeth in the 3rd and 8th sockets show resorption pits, the former with a small tooth bud laterally in the pulp cavity.

In the jaws, tooth implantation is of ankylothecodont type (Fig. 16) as summerised by Modesto and Sues (2004), in that the labial and lingual walls of the dental shelf of the tooth-bearing elements are rather tall (the lingual wall is slightly lower than the labial wall anteriorly and becomes even shorter posteriorly), and teeth are held in place by attachment tissue around their roots (Fig. 16B). The walls of the shelf are only weakly developed towards each other, not surrounding the teeth medially nor distally. An interdental plate is absent.

Fragments are present that might correspond to vertebral elements, but it is impossible to identify to which parts and to which vertebrae they belonged.

Stratigraphic and geographic range.—Induan (lowest Triassic) of South Africa.

Discussion

The reassessment of the cranial anatomy of the *Prolacerta broomi* (holotype, UCMZ 2003.41R) through CT scanning was able to correct several aspects of the anatomy given by Parrington (1935). The implications of these corrections and new retrieved data are discussed below, incorporating anatomical notes based on previous works on *Prolacerta* and closely related archosauromorphs. However, it is out of the scope of this work to present an extensive revision of the genus based on all the known materials of *Prolacerta* and its impact on the relationships of stem-archosaurs as this task is currently being undertaken by other researchers (Jonah Choiniere, personal communication 2020).

Other specimens.—The nasal articulations with the frontals are depicted as almost straight by Parrington (1935: fig. 1), but they are in fact smoothly concave anteriorly (Figs. 1A$_1$, 6). This is similar to BP/1/471 (Modesto and Sues 2004), but different from BP/1/5375 (Modesto and Sues 2004 mislabelled as BP/1/3575 in their figs. 7 and 8) and possibly also from UCMP 37151 (Camp 1945) and BPI 2675 (Gow 1975), where the nasals seem to laterally border antero-medial processes of the frontals, giving the contact a more U-shaped format.
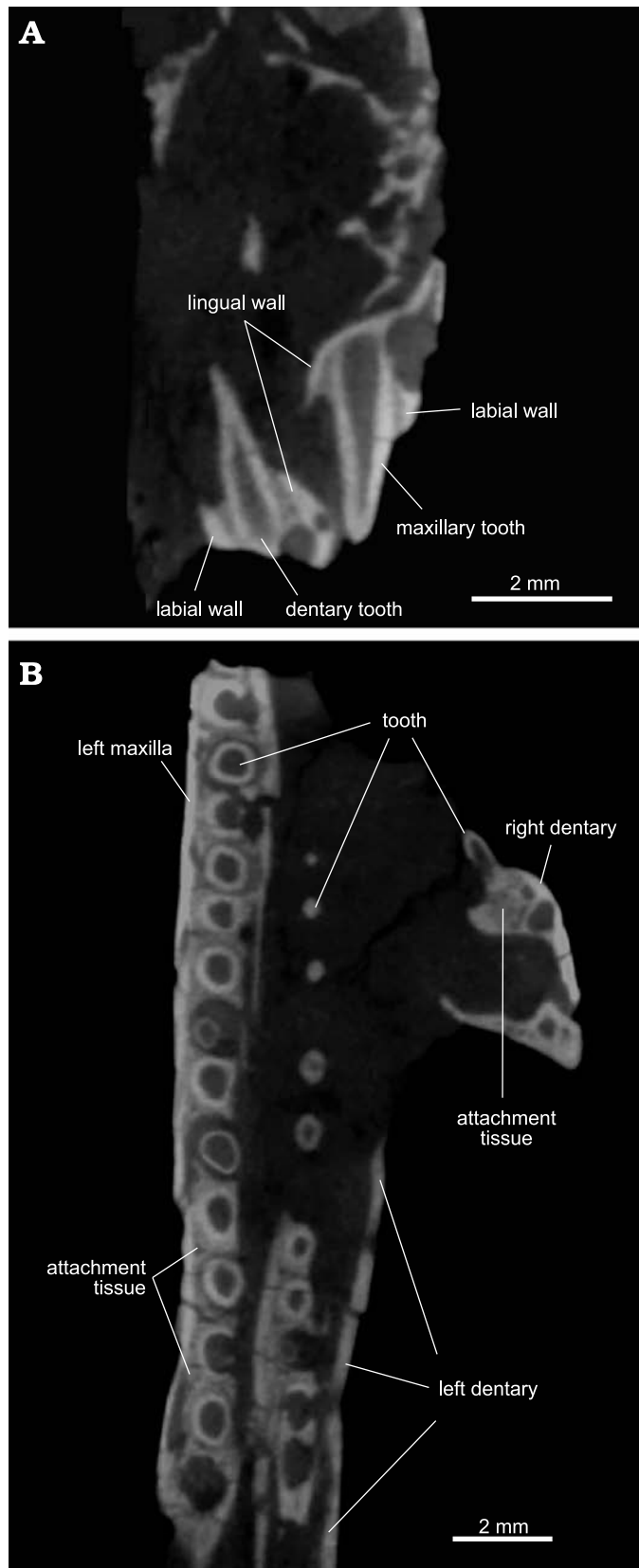
Fig. 16. Archosauromorph *Prolacerta broomi* Parrington, 1935, holotype UCMZ 2003.41R from Katberg Formation, *Lystrosaurus* Assemblage Zone, Karoo Basin; Induan, Lower Triassic; Harrismith Commonage, Free State, South Africa. Tooth implantation: **A**. 5th tooth socket of the dentary and 6th tooth socket of the maxilla with corresponding teeth in coronal section. **B**. Transverse section of the left maxillary and dentary tooth rows and a coronal section of a right dentary tooth. Anterior to the top in B.

Scan segmentation showed that the element identified as the left lacrimal by Parrington (1935: fig. 1) is part of the prefrontal. While the lacrimal and prefrontal do contact one another in UCMZ 2003.41R, the posterior part of the lacrimal lies within the matrix and behind the maxilla, and is thus not visible externally in the material. The prefrontal in UCMZ 2003.41R is restricted to the orbital margin, with no indication that the anterior flange would extend much further anteriorly. In no *Prolacerta* specimen is the prefrontal complete, so that the real anterior extension of the bone is unknown. In some, however, the prefrontal seems to have a more developed anterior flange than the one identified here, such as AMNH 9520 (Spiekman 2018), BP/1/471 and BP/1/5375 (Modesto and Sues 2004), while others conform with the holotype, like BPI 5066 (Modesto and Sues 2004).

The frontoparietal suture is very difficult to trace completely, and a contact between postfrontal and parietal is difficult to ascertain. On the right side, where all elements are in place, the posterolateral process of the frontal looks short. Thus, although the posterior process of the postfrontal does not seem to reach far enough posteriorly, a contact between it and the parietal is possible (Fig. 6). On the left side, however, the posterolateral process of the frontal seems more complete and longer. Nonetheless, the postfrontal is not preserved and the postorbital is not in place on this side. There is an articulation facet on the parietal (Fig. 6A$_2$), but whether this would have served the postfrontal alone or could have accommodated the postorbital as well is unclear. In any case, if present, the contact between postfrontal and parietal must have been at most very limited. This contrasts with what has been described for the holotype by Parrington (1935), and for other *Prolacerta* material (Camp 1945; Modesto and Sues 2004), where this contact is described as more extensive.

The quadrate is described as being overlain by the ventral process of the squamosal by Modesto and Sues (2004), but in UCMZ 2003.41R their relationship is more of a simple contact because the lateral flange of the quadrate is greatly abbreviated and does not extend beyond the tympanic crest (Fig. 7). In posterior view, it is the quadrate that partially covers the ventral ramus of the squamosal. I find it very unlikely to be a bias of preservation because the curvature of the lateral flange surface is very strong on both sides, directing the crest more laterally than anteriorly. Likewise, the quadratojugal is said to sheath the quadrate crest by Modesto and Sues (2004), but in UCMZ 2003.41R they do not overlap each other, except in posterior view, where the quadrate lateral flange covers part of the quadratojugal (Fig. 7B$_2$).

The articulation between quadrate and quadratojugal in UCMZ 2003.41R closely matches the description given for BPI 2675 by Gow (1975), in that it does not reach the distal end of the quadrate. It also conforms with many other *Prolacerta* specimens (Modesto and Sues 2004), but contrasts with the anatomy of SAM-PK-K10797 given by Ezcurra (2016), in that the quadratojugal not only reaches, but partially overlaps the quadrate distal end.

The identity of the element described by Parrington (1935) as the septomaxilla is unclear, but considering the element position in his figure 1, it seems to correspond to a fragment of the left side of the palate. Given its position, and comparing with the right side, it might correspond to the maxillary articulation of the palatine (Figs. 1A$_2$, 8). Likewise, the prevomer described by Parrington (1935) could be part of the anterior process of the vomer sticking out of the matrix. Camp (1945) also describes a prevomer for UCMP 37151, but although UCMZ 2003.41R cannot exclude the presence of a prevomer, this element is usually not present in reptilians.

The presence of medially directed teeth on the medial margin of the pterygoid has been described for UWBM 95529 (Spiekman 2018), and a row of "fang-like teeth" on the medial edge of the pterygoid reported for *Prolacerta* (Ezcurra 2016). These traits are not present in UCMZ 2003.41R. The presence and alignment of the tooth rows on the ventral surface of the pterygoid of UCMZ 2003.41R resemble closely that of BP/1/5066 (Modesto and Sues 2004), in which one row is found on the posterior edge of the transverse flange, the second trends antero-laterally, and the third extends anteriorly on the medial margin of the bone. Although the palate of UCMZ 2003.41R is slightly worn out, the medial row shows two lines of teeth, the lateralmost of which bears bigger teeth than the medial one, but which are directed posteriorly, not medially. The preserved portion of the ascending flange of the anterior ramus of the pterygoid also shows no sign of teeth. Spiekman et al. (2021: character 104) argued that the fourth tooth row of Ezcurra (2016) might in fact represent an extra, more medially positioned line of teeth belonging to the third row in a twisted anterior palatal ramus. Whatever the case, neither medially directed teeth, a fourth tooth row, nor an extra tooth line is present throughout the entire preserved length of the pterygoid of UCMZ 2003.41R.

The ectopterygoid is in articulation with the pterygoid on the left side of UCMZ 2003.41R and while it mostly agrees with what is known of the ectopterygoid in other specimens, it is important to mention that it articulates with the lateral flange of the pterygoid anteriorly as well as laterally, contrasting with the anterior-only articulation shown for BPI 2675 by Gow (1975).

The ventral surface of the basisphenoid of UCMZ 2003.41R is intermediate in morphology between that of BPI 2675 (Evans 1986) and UCMP 37151 (Camp 1945), being thus more similar to BPI 5066 (Modesto and Sues 2004) and UWBM 95529 (Spiekman 2018). The holotype does not show a deep parabolic depression between the cristae ventrolaterales as in UCMP 37151 (Camp 1945), nor does it show such a flat furrow as that of BPI 2675 (Evans 1986). The parasphenoid crest is also not well-marked and expanded laterally as in BPI 2675 (Evans 1986), and the cristae ventrolaterales not as sharp. It is unlikely that the basioccip-

ital would fill in the area between the cristae, as suggested by Parrington (1935) because in other archosauriforms, this area corresponds to the medial pharyngeal recess, and is formed mostly by the parabasisphenoid (Sobral et al. 2016; Sobral and Müller 2019). It is unclear why such differences exist in the parabasisphenoid of *Prolacerta*. One possibility is that they result from ontogeny. For instance, the pterygoid facets of the basipterygoid processes are more well-marked in BPI 2675 (Evans 1986) and the dorsum sellae and the articulation facet for the prootic more well-developed on the dorsal surface of the parabasisphenoid. In contrast, the processes are smoother in UCMZ 2003.41R, even though the facets are identifiable. The dorsum sellae are weakly developed and the prootic facets are not present. Nonetheless, the dorsal surface of the parabasisphenoid of UCMZ 2003.41R is not well-preserved, and these differences could be due to preservational bias.

The prootic of UCMZ 2003.41R is different from BPI 2675 (Gow 1975; Evans 1986) in which the ventral extension of the anterior inferior process of the prootic is proportionally longer than in BPI 2675. It is unlikely that this portion could belong to the parabasisphenoid, as it is present on both prootics and the dorsal part of the parabasisphenoid is not damaged on its articulation facet with the prootic. The braincase in UCMZ 2003.41R is overall not well-preserved, so that the significant of these differences might be overestimated. What Parrington (1935) described as the left paroccipital process is in fact the right one.

The lower jaw of UCMZ 2003.41R reveals several anatomical elements that remained mostly unknown for *Prolacerta* until now, such as the splenial and the prearticular. However, it was not able to elucidate some other, contentious morphological aspects like the extent of the contact between dentary and surangular. The area where these bones contact with one another and with the angular is damaged in UCMZ 2003.41R, but, as preserved, the dentary seems to have a more equal contact with both other bones, as pointed by Modesto and Sues (2004). What had been unknown thus far, however, is the lateral exposure of the splenial, and its possible participation in this contact (Fig. 15A$_1$). A contact between dentary and coronoid, as suggested by Modesto and Sues (2004), is likely medially, but a posterior extension of the former up to the coronoid eminence laterally is less certain. On the one hand, an articulation facet for the dentary on the surangular could not be confirmed in UCMZ 2003.41R, but, on the other hand, a very thin strip of bone extending posteriorly at the mid-height of the quadrate indicates that the bone extended further posteriorly than the last mandibular tooth (Fig. 15A$_1$). Unfortunately, it is not possible to clarify whether the dentary posterior extension would more closely resemble the reconstruction of Ezcurra (2016) or Spiekman (2018).

The posterior extension of the angular is also debated. Gow (1975) states that the angular reaches as far posteriorly as the glenoid fossa, contributing to it. This also seems to be the interpretation of Ezcurra (2016: fig. 29), but based on

UCMP 37151, Modesto and Sues (2004: 345) describe the angular as excluded from "more than half of the floor of the adductor fossa", being thus restricted to its anterior portion. In UCMZ 2003.41R, the ventromedial borders of the surangular and prearticular complement each other for the whole extension of the retroarticular process, thus completely excluding the angular from the glenoid fossa, but allowing it to participate in all, or most, of the adductor fossa. The posterior extension of the angular is thus as preserved, and the posteriormost part of the bone is not missing.

The lower jaw of *Prolacerta* is usually reconstructed as having a low coronoid region (Ezcurra 2016: fig. 29). Modesto and Sues (2004) also described the eminence as shallow, but their illustration of BP/1/471 indicates otherwise. This interpretation is probably due to the fact that most lower jaw material of *Prolacerta* is crushed and/or partially concealed by the rest of the skull, and the assumption that the coronoid bone in BP/1/471 indicated a higher dorsal margin of the lower jaw between the alveolar region and the coronoid eminence. However, segmentation of the right mandibular ramus of UCMZ 2003.41R clearly shows that this region was indeed well-developed (see below). A well-developed coronoid bone with posterodorsal and posteroventral processes was depicted for BPI 2675 by Gow (1975: fig. 20), although in UCMZ 2003.41R both processes are more prominent.

The type of tooth implantation in *Prolacerta*, and of basal archosauromorphs in general, has been a matter of extensive debate which is not intended to be covered in depth here. However, CT scans of UCMZ 2003.41R can shed some light on the issue. The alveoli of UCMZ 2003.41R show well-developed labial and lingual walls, but the sockets are not delimited medially nor distally by bone. The teeth do not sit free within these sockets, but the roots are surrounded by a distinct attachment tissue, the exact nature of which would have to be clarified by histological sections, confirming the interpretation of Nesbitt (2011). Resorption pits are present in several teeth, with examples of the existence of concomitant replacement teeth growing inside, contradicting Modesto and Sues (2004: 348), who state that "the lingual walls of the tooth-bearing bones are not modified during tooth replacement".

Finally, scans show that the element present just posterior to the left quadrate is the right exoccipital, and Parrington (1935) may have confused it for a vertebral centrum. The element posterior to the left squamosal is the opisthotic.

Taxonomy.—It was not possible to confirm some of the diagnostic features of the skull of *Prolacerta broomi* in the present study, such as the presence of a septomaxilla and a maxilla with long horizontal dorsal margin and concave posterior margin. Additionally, no medially directed teeth on the pterygoid medial margin was found, and thus this character is considered incorrect. Regarding the lower jaw characters newly added to the diagnosis, some comments are necessary.

It is unclear what the anatomy of the coronoid bone looks like in basal archosauromorphs, since this element is only rarely preserved. In *Macrocnemus bassanii*, where it is known among basal archosauromorphs, the coronoid is a strip of bone located on the dorsal margin of the lower jaw (Miedema et al. 2020). In this sense, the coronoid bone of *Prolacerta* resembles more closely that of basal lepidosauromorphs. In *Gephyrosaurus* (Evans 1980), the coronoid bone is also robust, albeit lacking a well-marked posterodorsal process, whereas in *Marmoretta* (Evans 1991) the process is well-developed. In both these taxa, the coronoid bone shows a distinct coronoid process, which is lacking in *Prolacerta*. A coronoid process in the coronoid bone is also found in *Macrocnemus bassanii* (Miedema et al. 2020).

The splenial is equally rarely described for basal archosauromorphs and its anatomical relationships on the medial side of the mandibular ramus only seldomly discussed. The splenial of UCMZ 2003.41R is similar to the one of *Macrocnemus bassanii* (Miedema et al. 2020) and *Tanystropheus longobardicus* (Nosostti 2007). In these taxa, the splenial is plate-like, forming most of the lingual wall of the lower jaw and wrapping around the mandibular ramus ventrally, being exposed for a good extent in lateral view. In *Mesosuchus*, the splenial is also visible laterally (Dilkes 1998), but its medial morphology is currently unknown. This anatomy could have a biomechanical origin beside a phylogenetic one, because in *Tanystropheus hydroides* (Spiekman et al. 2020) and in derived archosauriforms such as *Euparkeria* (Sookias et al. 2020), the splenial does not participate in the ventral margin of the lower jaw, being restricted to the medial wall of the mandible and thus not visible laterally. Although the splenial is visible externally for a short extension, the exact condition is unclear in *Teyujagua* (Pinheiro et al. 2019).

Snout anatomy.—The preserved region of the snout in UCMZ 2003.41R is difficult to interpret due to breakage and displacements of some of the bones. Additionally, the absence of the anterior extent of the prefrontal or of the articulation with the palatine complicates the interpretation of the many structures are found in this area.

Following the nomenclature of Benoit et al. (2021), sections 1 and 2 of the maxillary canal are not present in UCMZ 2003.41R because the anteriormost portion of the maxilla is not preserved on the left side and, on the right, these structures are damaged. Because the canal is not only formed by the maxilla, I will refer to it as the more classic dorsal alveolar canal (Oelrich 1956; Porter and Witmer 2015). Section 4 of the canal is delimited anteriorly by the posterior alveolar canal (Fig. 3A$_2$). As preserved, the lacrimal is slightly sigmoid in shape in dorsal view, so that its postero-lateral portion abuts to the medial side of the dental shelf of the maxilla. It would thus form the medial wall of the dorsal alveolar canal in a condition similar to that found in *Captorhinus laticeps* (Heaton 1979). However, the area is damaged, and if this relationship is not natural, then the lacrimal could have been positioned more laterally in vivo, in a condition more similar to *Orovenator* (Ford and Benson 2018), and this section would have been a medially open groove. In the *Prolacerta* specimen UCMP 37151, section 4 of the canal terminates posteriorly in a series of small foramina (Benoit et al. 2021: 391). In contrast, there is currently no indication that the canal bifurcates in UCMZ 2003.41R, even though participation of the palatine in the posteriormost section of section 4 is unknown (Porter and Witmer 2015). Finally, section 3 of the canal trends entirely within the maxilla, although its anteriormost limit is difficult to determine. In UCMP 37151, it is delimited by an "anterior medial [or internal] foramen for the superior alveolar nerve" that is located "on the rostrolateral margin of the maxillary sinus" (Benoit et al. 2021). This foramen seems to be present in BP/1/2675 as pictured by Gow (1975), but no such element was found in UCMZ 2003.41R. A crack trends through the material between the 2nd and 3rd tooth sockets and a small medial opening is present here. At about the same level in cross-section, there is a nutrient foramen on the lateral surface of the maxilla. There is, thus, the possibility that the medial opening was not caused by the crack and that it indeed corresponds to the anterior medial foramen, although much reduced in diameter compared to the posterior one.

A medial cavity is present on the medial surface of the maxilla in UCMZ 2003.41R (Fig. 3A$_2$), delimited anteriorly by the medial buttress of the maxilla and postero-dorsally by the ventral ridge of the nasolacrimal canal. Due to damage to the lacrimal, however, it is not possible to determine with certainty whether a nasolacrimal canal would be connected to the medial cavity.

A series of canals of different diameters are found within the lacrimal, two of which are prominent because of their thickness (approximately 0.6–0.7mm). They start posteriorly as two different foramina on the posterior surface of the lacrimal, one dorsal to the other. At about the posterior third of the bone, the ventral canal heads dorsally and seems to the merge with the dorsal canal. As the area is damaged, a medial opening of the ventral canal just before heading dorsally may be artificial, even though the medial surface of the lacrimal anterior to this seems to possess a recess that could indicate the anterior course of a branch, roofed by the ventral ridge of the nasolacrimal canal. The common, dorsally located canal continues anteriorly until about the anterior third of the lacrimal, where it then turns ventrally, leaving the bone through a foramen that opens at the end of a trough formed by the anterior bifurcation of the lacrimal (Fig. 3A$_2$). Several other, thinner canaliculi (about 0.2–0.3 mm thick) are found within the lacrimal, but due to damage it is very hard to reconstruct them digitally. Two of them seem to trend parallel, and very close, to the main canals, a ventral canaliculus ventral to the ventral canal and a dorsal canaliculus dorsal to the dorsal canal. The postero-lateral wall of the dorsal canal is open and the same might have been true for the ventral canal, although damage does not allow

certainty, thus matching the description of Gow (1975) and Modesto and Sues (2004).

The medial surface of the lacrimal dorsal to the common dorsal canal is recessed, which could indicate the course of a third canal, apparently without connection to the other two. This recessed area connects to an opening formed by the lacrimal laterally and by the anterior flange of the prefrontal medially in posterior view (Fig. 3A$_3$). A lacrimal apparatus with more than one main duct is found in the extant lizard *Varanus bengalensis* (= *V. monitor*, Bellairs 1949), in which the two ducts do not communicate with each other. In this case, the dorsal duct is broader and the canal is formed by the lacrimal and prefrontal, while the ventral one lies within the lacrimal entirely to some extent and, more anteriorly, on the medial surface of the maxilla, dorsal to the palatal shelf. This anatomy seems to correspond to what is found in UCMZ 2003.41R (Fig. 3A$_2$), although in *V. bengalensis* (Bellairs 1949) the two ducts are more unequal in size than the ones found in UCMZ 2003.41R.

Phylogenetic analysis

The phylogenetic relationships of *Prolacerta* are not yet completely settled, and currently there are two major understandings about its role in the early evolution of archosauromorphs. The first is that *Prolacerta* is a basal archosauromorph representing an earlier radiation than Tanystropheidae or Crocopoda (Spiekman et al. 2021); and the second is that *Prolacerta* is found more crownward than the former and nested well within the latter, being closely related to *Teyujagua* + Archosauriformes (Ezcurra and Sues 2021). In order to test the impact of these new anatomical information retrieved from UCMZ 2003.41R on the phylogenetic placement of *Prolacerta*, the holotype was incorporated into these two recent analyses.

Adding the holotype as a new terminal in the dataset of Ezcurra and Sues (2021) retrieves it within Prolacertidae, collapsed with *Boreopricea* and with *Prolacerta* + *Kadimakara* (Fig. 17A). Removing the *Prolacerta broomi* taxon from the
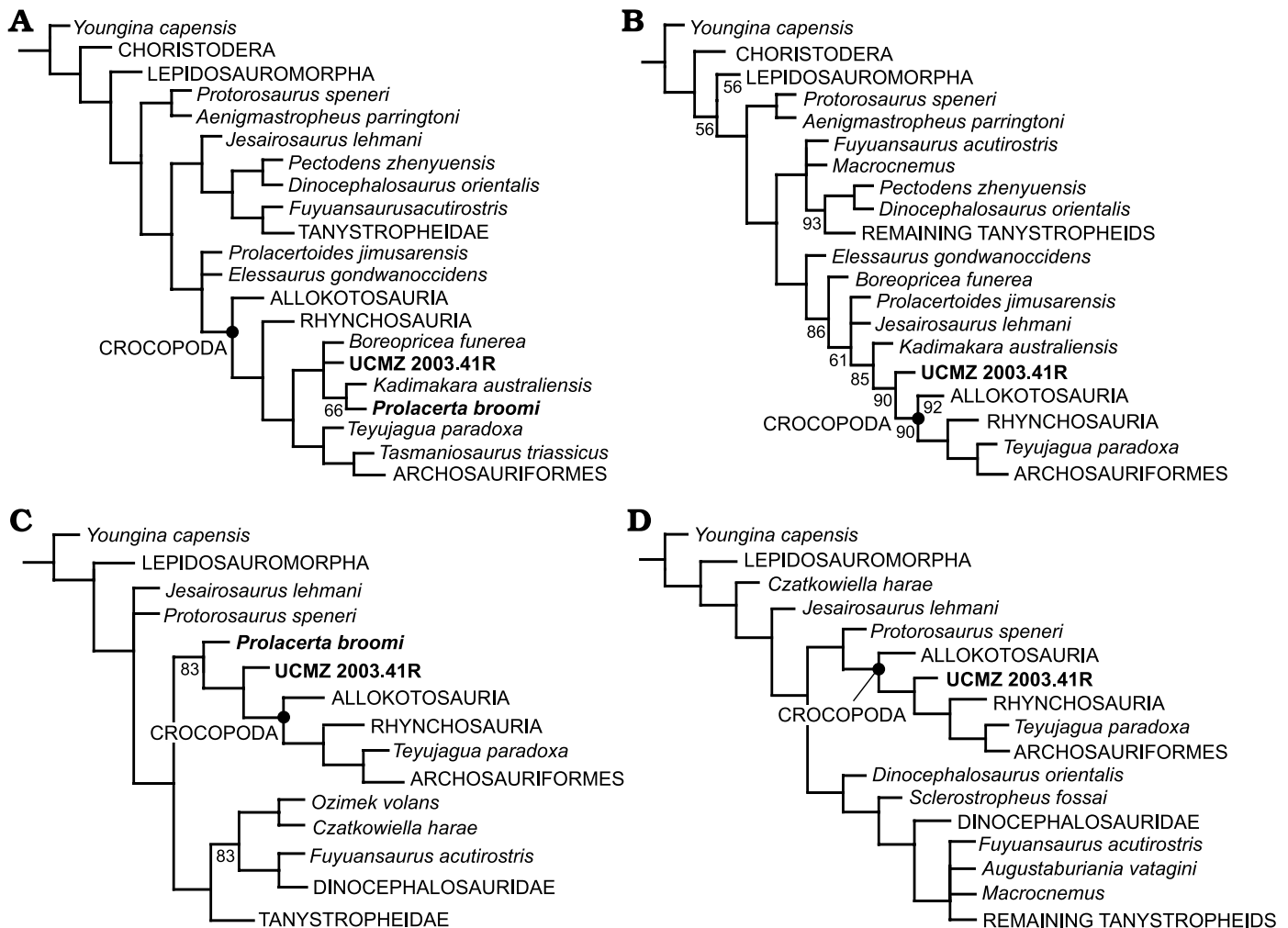

Fig. 17. Majority rule consensus trees depicting the phylogenetic relationships of the *Prolacerta broomi* Parrington, 1935, holotype UCMZ 2003.41R. Analyses of Ezcurra and Sues (2021): UCMZ 2003.41R as an independent addition to the data matrix (**A**) and as the single taxon representing the *Prolacerta* (**B**). Analyses of Spiekman et al. (2021): UCMZ 2003.41R as an independent addition to the data matrix (**C**) and as the single taxon representing the *Prolacerta* (**B**). Numbers under branches represent their occurrence frequency.

dataset shows UCMZ 2003.41R in a more basal position, as the sister taxon of Crocopoda (Fig. 17B). In this scenario, the remaining prolacertids are also pulled down towards the root of Archosauromorpha without forming a monophyletic family, but as successive sister taxa to UCMZ 2003.41R + Crocopoda. It also attracts *Jesairosaurus* out of the tanystropheid lineage and into these successive sister groups of Crocopoda. Incorporating UCMZ 2003.41R to the analysis of Spiekman et al. (2021) also retrieves it as the sister taxon of Crocopoda and moves the taxon *Prolacerta broomi* up the tree, making it more closely related to Crocopoda than to Tanystropheidae or Dinocephalosauridae (Fig. 17C). Analysing UCMZ 2003.41R alone in the same setting will result in the holotype being more derived than Allokotosauria (Fig. 17D), showing it as sister to (Rhynchosauria (*Teyujagua* + Archosauriformes)). In this setting, *Protorosaurus* is also attracted to the crocopod lineage.

In none of the analyses where UCMZ 2003.41R is incorporated as an independent OTU is it found as the sister taxon of the existing *Prolacerta* OTU, which may indicate that an anatomical incongruence among the holotype and the other known *Prolacerta* specimens exist. Whether these incongruences reflect a more profound taxonomic inconsistency remains to be explored and, as already mentioned, is out of the scope of this work. It is also interesting to notice that in the analyses of both datasets where UCMZ 2003.41R is considered alone, it is retrieved close to the origin of Crocopoda, and that in none of these cases is UCMZ 2003.41R found as more derived than Rhynchosauria. Such a relationship with rhynchosaurs has been explored in an evolutionary scenario considering the braincase anatomy, in which the overall morphology seen in BPI 2675, whose anatomical aspects are now mostly confirmed in UCMZ 2003.41R, is more similar to that of *Youngina* (Gardner et al. 2010) than to *Mesosuchus* (Sobral and Müller 2019). The overall conclusion in these phylogenetic analyses is that UCMZ 2003.41R is pulled down the archosauromorph tree in the dataset of Ezcurra and Sues (2021) and it is pushed up in the one of Spiekman et al. (2021).

Conclusions

Despite of being a very important model for the early evolution of crown-diapsids, the holotype specimen of *Prolacerta broomi* had never been re-visited since its first description by Parrington (1935). Through the application of CT-scanning techniques, it was possible to update several aspects of the anatomy of the holotype and to add new information on previously unknown elements of the material, contributing to the anatomical diversity found in the genus *Prolacerta*. For instance, the articulation between nasals and frontals are anteriorly concave in UCMZ 2003.41R, being similar to some *Prolacerta* specimens but different from others, where it is anteriorly convex. The contact between postfrontal and parietal is more likely absent in UCMZ 2003.41R, in con-

trast to other specimens where it is present. The quadrate of UCMZ 2003.41R is not covered by the squamosal laterally, not by the quadratojugal ventrally. The pterygoid of UCMZ 2003.41R does not bear medially directed teeth nor a fourth tooth row as suggested by previous analyses (Ezcurra 2016; Spiekman et al. 2021). In UCMZ 2003.41R, the basisphenoid ventral surface is intermediate in anatomy between the flat furrow described for BPI 2675 (Evans 1986) and the deep parabolic depression of UCMP 37151 (Camp 1945).

The internal anatomy of both the lower jaw and the snout were substantially revised. The splenial is confirmed to form most of the lingual side of the lower jaw, as well as the mandibular ramus ventrally, while the lateral exposure of the angular seems not to have been as extensive as described for other *Prolacerta* specimens. The coronoid bone of UCMZ 2003.41R shows prominent posterodorsal and posteroventral processes, different from other known basal archosauromophs but similar to basal lepidosauromorphs. The glenoid and adductor fossae of the mandible are shallow and medially open. The tooth sockets of UCMZ 2003.41R are incomplete, in the sense that they lack medial and distal walls. However, the teeth are held in place by an attachment tissue, as interpreted by Nesbitt (2011). Resorption pits are present in several teeth.

The orbitonasal region of early reptiles has received some attention recently for its importance in systematics of the group (Benoit et al. 2021), and even though *Prolacerta* has been extensively used as a diapsid model, descriptions of the region are still limited, and no comparisons have been made with the holotype. The orbitonasal region of UCMZ 2003.41R closely resembles the anatomy described for *Orovenator* (Ford and Benson 2018), even though some aspects of it, such as the contribution of the lacrimal to the dorsal alveolar canal, is more similar to *Captorhinus* (Heaton 1979). However, there is some morphological variation in some aspects of the dorsal alveolar canal, given UCMZ 2003.41R seems to differ from UCMP 37151 in its posterior aspect, the former not being bifurcated as the latter. The presence of the anterior medial foramen was also not confirmed in UCMZ 2003.41R. The anteriormost aspect of this canal, as well as the entire morphology of the medial sinus could not be assessed in UCMZ 2003.41R due to lack of preservation.

It is out of the scope of this work to compare all the *Prolacerta* specimens in a broader taxonomic review, as this is currently under work elsewhere. However, the addition of UCMZ 2003.41R as an independent OTU in two recently published archosauromoph matrices does not retrieve the holotype specimen as sister group to existing *Prolacerta* scorings, potentially indicating an anatomical incongruence among known *Prolacerta* material. The aim of this study was for this anatomic review of the holotype material of *Prolacerta,* together with the newly added information on its skull morphology, to facilitate further studies of the genus and other archosauromorph comparative studies henceforth.

Acknowledgements

References

Bellairs, A.A. 1949. Observations on the snout of *Varanus*, and a comparison with that of other lizards and snakes. *Journal of Anatomy* 83: 116–146.

Benoit, J., Ford, D.P., Miyamae, J.A., and Ruf, I. 2021. Can maxillary canal morphology inform varanopid phylogenetic affinities? *Acta Paleontologica Polonica* 66: 389–393.

Benton, M.J. 1985. Classification and phylogeny of the diapsid reptiles. *Zoological Journal of the Linnean Society* 118: 261–308.

Benton, M.J. and Allen, J.L. 1997. *Boreopricea* from the Lower Triassic of Russia, and the relationships of the prolacertiform reptiles. *Palaeontology* 40: 931–953.

Brinkman, D. 1981. The origin of the crocodyloid tarsi and the interrelationships of thecodontian archosaurs. *Breviora* 464: 1–23.

Broom, R. and Robinson, J.T. 1948. Some new fossil reptiles from the Karoo Beds of South Africa. *Journal of Zoology* 118: 392–407.

Camp, C.L. 1945. *Prolacerta* and the protosaurian reptiles. *American Journal of Sciences* 243: 17–32.

Chatterjee, S. 1986. *Malerisaurus langstoni*, a new diapsid reptiles from the Triassic of Texas. *Journal of Vertebrate Paleontology* 64: 297–312.

Colbert, E.H. 1987. The Triassic reptile *Prolacerta* in Antarctica. *American Museum Novitates* 2882: 1–19.

Dilkes, D.W. 1998. The Early Triassic rhynchosaur *Mesosuchus browni* and the interrelationships of basal archosauromorph reptiles. *Philosophical Transactions of the Royal Society of London* 353: 501–541.

Evans, S.E. 1980. The skull of a new eosuchian reptile from the Lower Jurassic of South Wales. *Zoological Journal of the Linnean Society* 70: 203–264.

Evans, S.E. 1986. The braincase of *Prolacerta broomi* (Reptilia; Triassic). *Neues Jahrbuch für Geologie und Paläontologie Monatshefte* 1986 (4): 193–203.

Evans, S.E. 1988. The early history and relationships of the Diapsida. *In*: M.J. Benton (ed), *The Phylogeny and Classification of Tetrapods, Vol 1: Amphibians, Reptiles, Birds*, 221–260. Clarendon Press, Oxford.

Evans, S.E. 1991. A new lizard-like reptile (Diapsida: Lepidosauromorpha) from the Middle Jurassic of England. *Zoological Journal of the Linnean Society* 103: 391–412.

Ezcurra, M.D. 2016. The phylogenetic relationships of basal archosauromorphs, with an emphasis on the systematics of proterosuchian archosauriforms. *PeerJ* 4: e1778.

Ezcurra, M.D. and Sues, H.-D. 2021. A re-assessment of the osteology and phylogenetic relationships of the enigmatic, large-headed reptile *Sphodrosaurus pennsylvanicus* (Late Triassic, Pennsylvania, USA) indicates archosauriform affinities. *Journal of Systematic Palaeontology* 19: 1643–1677.

Ezcurra, M.D., Scheyer, T.M., and Butler, R.J. 2014. The origin and early evolution of Sauria: reassessing the Permian saurian fossil record and the timing of the crocodilian-lizard divergence. *PLoS ONE* 9: e89165.

Ford, D.P. and Benson, R.B.J. 2018. A redescription of *Orovenator mayorum* (Sauropsida, Diapsida) using high-resolution μCT, and the consequences for early amniote phylogeny. *Papers in Palaeontology* 2018: 1–43.

Gardner, N.M., Holliday, C.M., and O'Keefe, F.R. 2010. The braincase of *Youngina capensis* (Reptilia, Dipsida): new insights from high-resolution CT scanning of the holotype. *Palaeontologia Electronica* 13 (3): 19A.

Gow, C.E. 1975. The morphology and relationships of *Youngina capensis* Broom and *Prolacerta broomi* Parrington. *Palaeontologia Africana* 18: 89–131.

Groenewald G.H. and Kitching J.W. 1995. Biostratigraphy of the *Lystrosaurus* Assemblage Zone. *In*: B.S. Rubidge (ed.), Biostratigraphy of the Beaufort Group (Karoo Supergroup). *Pretoria: South African Committee for Stratigraphy, Biostratigraphic Series* 1: 35–39.

Heaton, M.J. 1979. Cranial anatomy of the primitive captorhinid reptiles from the Late Pennsylvanian and Early Permian, Oklahoma and Texas. *Bulletin of the Oklahoma Geological Survey* 127: 1–80.

Martínez, R.N., Simões, T.R., Sobral, G., and Apesteguía, S. 2021. A Triassic stem lepidosaur illuminates the origin of lizard-like reptiles. *Nature* 597: 235–238.

Modesto, S.P. and Sues, H.-D. 2004. The skull of the Early Triassic archosauromorph reptile *Prolacerta broomi* and its phylogenetic significance. *Zoological Journal of the Linnean Society* 140: 335–351.

Müller, J. 2004. The relationships among diapsid reptiles and the influence of taxon selection. *In*: G. Arratia, M.V.H. Wilson, and R. Cloutier (eds), *Recent Advances in the Origin and Early Radiation of Vertebrates*, 379–408. Verlag Dr. Friedrich Pfeil, München.

Miedema, F., Spiekman, S.N.F., Fernandez, V., Reumer, J.W.F., and Scheyer, T.M. 2020. Cranial morphology of the tanystropheid *Macrocnemus bassani* unveiled using synchrotron microtomography. *Scientific Reports* 10: 12412.

Nesbitt, S.J. 2011. The early evolution of archosaurs: relationships and the origin of major clades. *Bulletin of the American Museum of Natural History* 352: 1–292.

Nesbitt, S.J., Flynn, J.J., Pritchard, A.C., Parrish, J.M., Ranivoharimanana, L., and Wyss, A.R. 2015. Postcranial osteology of *Azendohsaurus madagaskarensis* (?Middle to Upper Triassic, Isalo Group, Madagascar) and its systematic position among stem archosaur reptiles. *Bulletin of the American Museum of Natural History* 398: 1–126.

Nosotti, S. 2007. Tanystropheus longobardicus (Reptilia, Protorosauria): re-interpretations of the anatomy based on new specimens from the Middle Triassic of Besano (Lombardy, Northern Italy). *Memorie della Societa Italiana di Scienze Naturali e del Museo Civico di Storia Naturale di Milano* 35: 1–88.

Oelrich, T.M. 1956. The anatomy of the head of *Ctnosaura pectinata* (Iguanidae). *Miscellaneous Publications Museum of Zoology University of Michigan* 94: 1–122.

Parrington, F.R. 1935. On *Prolacerta broomi*, gen. et sp. n. and the origin of lizards. *Annals and Magazine of Natural History* 16: 197–205.

Pinheiro, F.L., Simão-Oliveira, D., and Butler, R.B. 2019. Osteology of the archosauromorph *Teyujagua paradoxa* and the early evolution of the archosauriform skull. *Zoological Journal of the Linnean Society* 189 (1): 378–417.

Porter, W.R. and Witmer, L.M. 2015. Vascular patterns in iguanas and other squamates: blood vessels and sites of thermal exchange. *PLoS ONE* 10: e0139215.

Rieppel, O., Fraser, N.C., and Nosotti, S. 2003. The monophyly of Protorosauria (Reptilia, Archosauromorpha): a preliminary analysis. *Atti della Societa Italiana di Scienzi Naturali e del Museo Civico di Storia Naturale di Milano* 144: 359–382.

Romer, A.S. 1966. *Vertebrate Paleontology. 3rd Edition*. 468 pp. University of Chicago Press, Chicago.

Senter, P. 2004. Phylogeny of the Drepanosauridae (Reptilia: Diapsida). *Journal of Systematic Palaeontology* 2: 257–268.

Sobral, G. and Müller, J. 2019. The braincase of *Mesosuchus browni* (Rep-

tilia, Archosauromorpha) with information on the inner ear and description of a pneumatic sinus. *PeerJ* 7: e6798.

Sobral, G., Simões, T.R., and Schoch, R.R. 2020. A tiny new Middle Triassic stem-lepidosauromorph from Germany: implications for the early evolution of lepidosauromorphs and the Vellberg fauna. *Scientific Reports* 10: 2273.

Sobral, G., Sookias, R.B., Bhullar, B.-A.S., Smith, R., Butler, R.J., and Müller, J. 2016. New information on the braincase and inner ear of *Euparkeria capensins* Broom: implications for diapsid and archosaur evolution. *Royal Society Open Science* 3: 160072.

Sobral, G., Sues, H.-D., and Müller, J. 2015. Anatomy of the enigmatic reptile *Elachistosuchus huenei* Janensch, 1949 (Reptilia: Diapsida) from the Upper Triassic of Germany and its relevance for the origin of Sauria. *PLoS ONE* 10: e0135114.

Sookias, R.B., Dilkes, D., Sobral, G., Smith, R.M.H., Wolvaardt, F.P., Arcucci, A.B., Bhullar, B.-A.S., and Werneburg, I. 2020 The craniomandibular anatomy of the early archosauriform *Euparkeria capensis* and the dawn of the archosaur skull. *Royal Society Open Science* 7: 200116.

Spiekman, S.N.F. 2018. A new specimen of *Prolacerta broomi* from the lower Fremouw Formation (Early Triassic) of Antarctica, its biogeographical implications and a taxonomic revision. *Scientific Reports* 8: 17996.

Spiekman, S.N.F., Fraser, N.C., and Scheyer, T.M. 2021. A new phylogenetic hypothesis of Tanystropheidae (Diapsida, Archosauromorpha) and other "protorosaurs", and its implications for the early evolution of stem archosaurs. *PeerJ* 9: e11143.

Spiekman, S.N.F., Neenan, J.M., Fraser, N.C., Fernandez, V., Rieppel, O., Nosotti, S., and Scheyer, T.M. 2020. The cranial morphology of *Tanystropheus hydroides* (Tanystropheidae, Archosauromorpha) as revealed by synchrotron microtomography. *PeerJ* 8: e10299.

Wild, R. 1973. Die Triasfauna der Tessiner Kalkalpen XXIV. Neue Funde von *Tanystropheus* (Reptilia, Squamata). *Abhandlungen schweizeriches paläontologisches Gesellschaft* 95: 1–162.